NATIONAL ADVISORY COMMITTEE FOR AERONAUTICS

TECHNICAL MEMORANDUM

No. 1125

THE INFLUENCE OF THE DIAMETER RATIO ON THE CHARACTERISTICS DIAGRAM OF THE AXIAL COMPRESSOR

By B. Eckert, F. Pflüger, and F. Weinig

TRANSLATION

"Der Einfluss des Nabenverhältnisses auf das Kennfeld des Axialgebläses"

Forschungsinstitut für Kraftfahrwesen und Fahrzeugmotoren
Technische Hochschule Stuttgart

Washington
April 1948

NATIONAL ADVISORY COMMITTEE FOR AERONAUTICS

TECHNICAL MEMORANDUM NO. 1125

THE INFLUENCE OF THE DIAMETER RATIO ON THE CHARACTERISTICS DIAGRAM OF THE AXIAL COMPRESSOR*

By B. Eckert, F. Pflüger, and F. Weinig

Report from the Stuttgart Research Institute for Automobiles and Engines (="FKFS")

PREFACE

The hub diameter of axial-flow work machines is in the first place determined by the stage head and in the second place by the axial-flow velocity. Great pressures or heads in all cases require a large diameter ratio. On the other hand, particularly when very great volumes have to be handled, for example, in the first stage of axial compressors or in cooling fans, the hub must be small in order to avoid too great meridian velocities, capacity coefficients, that is, which would act detrimentally upon the efficiency of the work machine.

The following rule may be recommended for a first approximation: The lower limit of the diameter ratio is limited by the empirical equation $\upsilon \gtrapprox \sqrt{0.8\psi}$ dependent upon the pressure coefficient. A further lower limit for the size of the hub is set by the surging limit. According to the Institute's experience, we must have the throttling or quantity coefficient $\sigma = \frac{\varphi^2}{\psi} \gtrapprox 0.1$. We hereby obtain a second limiting condition for the smallest allowable diameter ratio

$$\upsilon \gtrapprox \sqrt{1 - \frac{\left(\frac{2}{D}\right)^2 \dot{V}}{\sqrt{2g\, H_{ad}}_{stage}}}$$

*"Der Einfluss des Nabenverhältnisses auf das Kennfeld des Axialgebläses." Forschungsinstitut für Kraftfahrwesen und Fahrzeugmotoren, Technische Hochschule Stuttgart.

With very great stage heads, great pressure coefficients, that is, or with small volumes, the diameter ratio on the basis of both aforementioned empirical equations becomes very large. The following investigations therefore are concerned in particular with the question of the upper limiting condition for the diameter ratio. It is hereby found that the question of the ratio of active blade surface to passive surface, that is, to the hub and housing walls, plays a decisive part in influencing the efficiency. To obtain the maximum efficiency an upper limiting condition $\upsilon \lesssim 0.9$ should not be exceeded, on the basis of the following results.

In case of necessity, the diameter ratio may be somewhat smaller than corresponds to the above lower limiting condition, this being based upon unequal pressure distribution over the blade radius; that is, the blade is loaded less at the hub and more at the outer cylindrical sections, to such an extent that the mean value of the total pressure behind the blade again corresponds to the required value.

SUMMARY

With the further development of axial blowers into highly loaded flow machines, the influence of the diameter ratio upon air output and efficiency gains in significance. Clarification of this matter is important for single-stage axial compressors, and is of still greater importance for multistage ones, and particularly for aircraft power plants. Tests with a single-stage axial blower gave a decrease in the attainable maximum pressure coefficient and optimum efficiency as the diameter ratio increased. The decrease must be ascribed chiefly to the guide surface of the hub and housing between the blades increasing with the diameter ratio.

SECTIONS

1. Introduction

2. Scope of tests and test procedure

3. Test results and evaluation of tests
   (a) The influence of the diameter ratio on the non-dimensional characteristics and design factors
   (b) Subdivision of the total efficiency, and the relation between the partial efficiencies and the diameter ratio
   (c) The influence of the diameter ratio on the drag-lift ratio

. Summary

INDEX OF THE FREQUENTLY USED SYMBOLS

c_a	lift coefficient (–)
c_m	mean flow velocity in the blower (m/s)
c_u	component in the peripheral direction; tangential component (m/s)
c_w	drag coefficient (–)
c_Γ	circulation coefficient (–)
$D = 2R$	blower outer diameter (m)
$d = 2r_i$	blower hub diameter (m)
r	distance of one blade element from the axis of rotation (m)
g	acceleration of gravity (m/s^2)
$\dot{G}$	weight flow (kg/s)
H	head (m)
K_n	nondimensional rotary speed (–)
k_l	power coefficient (–)
$k_{l_{vent}}$	windage power-loss coefficient (–)
$k_\epsilon = \frac{\epsilon_R}{\epsilon_P}$	cascade influence coefficient (–)
l	blade chord (m)

N_{total}	shaft power; total power (mkg/s)
N_m	mechanical power loss (mkg/s)
$N_i = \dot{G}H_{th}$	indicated compressor power (mkg/s)
$N_{R_{loss}} = \dot{G}H_{R_{loss}}$	power loss in the rotor blading (mkg/s)
$N_{L_{loss}} = \dot{G}H_{L_{loss}}$	power loss in the stator blading (mkg/s)
$N_{vent} = \dot{G}H_{vent}$	windage power loss (mkg/s)
$N_{vol} = \dot{G}H_{vol}$	clearance power loss (mkg/s)
$N_u = \dot{G}H_u$	rotor periphery power (power developed by blades) (mkg/s)
$N_{st} = \dot{G}H_{st}$	stage power (mkg/s)
$N_n = \dot{G}H_{ad}$	useful power (mkg/s)

See figure 22.

n	rotary speed of the compressor (rpm)
$\Delta p = \gamma H$	pressure rise (kg/m^2)
S	width of clearance (m)
t	blade spacing or pitch (m)
u	peripheral velocity (m/s)
$\dot{V}$	flow volume (m^3/s)
z	number of blades in the rotor (-)
β_s	angle between the peripheral direction and the chord of the profile center line, degrees
ϵ	drag-lift ratio (-)

ϵ_R rotor drag-lift ratio (-)

ϵ_p profile drag-lift ratio (-)

η efficiency (-)

υ diameter ratio (-)

ρ mass density (kgs^2/m^4)

γ volume density (kg/m^3)

φ compressor flow (or capacity) coefficient (-)

ψ compressor pressure coefficient (-)

σ throttling or quantity coefficient (-)

σ_∞ flow angle (angle between the mean relative approach velocity and the peripheral velocity), degrees

Subscripts:

mech mechanical

vol volumetric

vent windage

u blade

i_{ad} internal isentropic

ad = total over-all efficiency at the blower coupling

R rotor

L stator

z number of blades in the rotor (-)

β_s angle between the peripheral direction and the chord of the profile center line, degrees

ϵ drag-lift ratio (-)

m mean section

p profile

ad isentropic

∞ relative to the actual approach flow direction

a outer

i inner

Superscript:

for one blade element

1. INTRODUCTION

With low-pressure axial blowers, but also with axial blowers having pressure coefficients up to about $\psi = 0.3$, the influence of the diameter ratio on the blower characteristics is not particularly large. In this case the hub dimensions are usually so chosen that there may be room for the number of blades determined mathematically. With an increase in the stage pressure coefficient, which is desirable for various reasons, a knowledge of the capacity coefficient suitable for a prescribed pressure coefficient ψ is necessary, because upon falling short of a certain ratio between the capacity coefficient and the pressure coefficient expressed by the throttling or quantity coefficient $\sigma = \frac{\varphi^2}{\psi}$ the surge limit of a compressor is reached or passed, which makes perfect operation of the compressor out of question. However, because the capacity coefficient $\varphi = \frac{c_m}{u_a} = \frac{\dot{V}}{\frac{\pi}{4} D^2(1 - \upsilon^2)} \frac{1}{u_a}$ is decisively affected by the diameter ratio $\upsilon = \frac{d}{D}$ the allowable diameter ratio is of greater importance with blower having high pressure coefficients.

For this reason the problem exists of finding the dependence of the attainable quantity coefficient $\sigma = \frac{\varphi^2}{\psi}$ upon the diameter ratio,

of determining the effect of diameter ratio of various sizes upon the attainable blower efficiency, and of clarifying the magnitude of the diameter ratio's influence. Knowledge of the influence of the diameter is particularly important for multistage axial compressors, for aircraft engine superchargers, and for compressors for jet engines; for example, because with increasing compression the flow volume falls off, whereas the stage pressure increase on the other hand must remain as great as possible in order to manage with as few stages as possible. Under these circumstances it is chiefly knowledge of the diameter ratio $\upsilon > 0.7$ that is worth while.

2. SCOPE OF TESTS AND TEST PROCEDURE

The 48-blade axial rotor shown in figure 1 was used as an experimental blower and its blade sections and characteristic dimensions are shown in figure 2. Changing the cowls of the blower approach flow and blow-off, and of the following guide devices or stator (fig. 3) made it possible in a very simple way to investigate the diameter ratios between the limits $\upsilon = 0.75$ to 0.95. The rotors and stators of the experimental blower were calculated and built for the diameter ratio $\upsilon = \frac{0.34}{0.45} = 0.75$ and suitable inserts were provided for larger diameter ratios. Care was taken in this connection that the ineffective blade roots with the larger diameters could not falsify the result through additional windage losses. The static pressure measurements in front and behind the rotor and stator were taken both outside at the housing and also inside at the front and rear cowls; that is, at the outer and at the inner borders of the flow. (See fig. 3.) The pressure readings under these circumstances varied only very little from one another. In order to obtain measurement readings for various blade settings, the rotor blades were made adjustable. With the large number of blades it seemed expedient, in order to save time and to increase the accuracy of the tests, to be able to turn and lock all blades simultaneously, which was made possible by the toothed adjusting device shown in figure 1. The drive balls engaging the teeth of the adjusting device were installed with no play whatever.

3. TEST RESULTS AND EVALUATION OF TESTS

(a) The Influence of the Diameter Ratio on the Nondimensional Characteristics and Design Factors

Figures 4 to 8 show, for five different diameter ratios $\upsilon = 0.755$ 0.8, 0.85, 0.9, and 0.95 of the single-stage test blower, the experimentally found dependence of the revolutions per minute and the blower efficiency upon the capacity coefficient. From these blower characteristics diagrams, we clearly see that a decrease in the maximum revolutions per minute attainable and in the optimum efficiency accompanies an increase in the diameter ratio.

In order to make it possible to utilize the test results as a basis for further calculations, the influence of the diameter ratio was also represented in still another way as a function of a definitely determined nondimensional characteristic. In a way similar to the specific revolutions per minute for pumps and turbines, which serves as a basis for their belonging to a certain classification, we may also set up for axial-flow blowers a corresponding characteristic magnitude:[1]

$$K_n = 2\pi^{1/2} \frac{nV^{1/2}}{(2gH_{ad})^{3/4}} \quad (-) \qquad (1)$$

---

[1]Weber, M.: Die spezifischen Drehzahlen und die anderen Kenngrössen der Wasserturbinen, Kreiselpumpen, Windräder und Propeller als dimensionsfreie Kenngrössen der Ähnlichkeitsphysik. Schiffbau Bd. 31 (1930) pp. 73, 156, 207, 413, 432.

Weber, M.: Das allgemeine Ähnlichkeitsprinzip der Physik und sein Zusammenhang mit der Dimensionslehre und der Modellwissenschaft. Jahrb. d. Schiffbautechn. Ges. Bd. 31 (1930) p. 273.

Weinig, F.: Ein Vergleich zwischen Kolbenmaschinen und Tragflügelmaschinen mit Hilfe dimensionsloser Kenngrössen. Mot.-techn.Z. Bd. 2 (1940) H. 8 p. 255.

Eckert, B.: Dimensionslose Kenngrössen von Gebläsen und Verdichtern. Auto.-techn.Z. Bd. 47 (1944) H. 1/2 pp. 1 to 7.

Because the characteristics diagrams (figs. 4 to 8) are as usual plotted in nondimensional form, it is advantageous also to express the nondimensional rotary speed in the nondimensional design factors. We obtain with the flow volumes

$$\dot{V} = \varphi \pi R^2 (1 - \upsilon^2) u_a$$

for one time unit, and with the head

$$H_{ad} = \psi \frac{u_a^2}{2g}$$

the nondimensional rotary speed

$$K_n = \varphi^{1/2} (1 - \upsilon^2)^{1/2} \psi^{-3/4} \qquad (2)$$

The throttling or quantity coefficient is defined as the ratio of the dynamic pressure to the total pressure

$$\sigma = \frac{\Delta p_{dyn}}{\Delta p_{dyn} + \Delta p_{st}} = \frac{\left(\frac{\rho}{2}\right) c_m^2}{\Delta p_{tot}} \frac{\left(\frac{\rho}{2}\right) c_m^2}{\left(\frac{\rho}{2}\right) u_a^2} = \frac{\varphi^2}{\psi} \qquad (3)$$

Now if we insert into the separate blower characteristic diagrams the lines of constant nondimensional rotary speed (equation (2)) and constant quantity coefficients (equation (3)), then we obtain figures 9 to 13. From these graphs it is now possible to see the influence of the diameter ratio υ upon the characteristics φ, ψ, η, of an axial blower, and the connection with the important nondimensional characteristic magnitudes K_n and σ which determined the preliminary computations and the production design.

Figures 9 to 13 do indeed contain all knowledge gained in the present experiments; their use is however not very clear because of the subdivision into five separate diagrams, and because of the many dependent variables (φ, ψ, σ, η, K_n, β_s, υ). For these reasons a few particularly important results of evaluation will be discussed in the following.

If we think of the curves of specific rotary speed in figures 9 to 13 as tangents to the conchoidal efficiency curves, and connect the contact points together, then we obtain the optimum efficiency reached in the present experiments, for the case under consideration as a function of the nondimensional rotary speed for various diameter ratios (fig. 14). In figure 14, which contains the results for all five diameter ratios investigated, the corresponding lines of constant quantity coefficient are also drawn in.

The results show that with the usually prescribed nondimensional rotary speeds the attainable blower efficiencies decrease as the diameter ratio increases. This discovery goes beyond the investigated pitch ratio, and is of fundamental importance in the preliminary design of multistage axial compressors.

In the future still other pitch ratios, and particularly larger pitch ratios, are to be investigated; yet with such rotors only a small stage pressure increase will be reached, so that they are of minor significance for the multistage type.

Special attention must be drawn to the fact that with different compressors under consideration, numerical values should not be taken from figure 14; figure 14 is intended merely to illustrate in a general way that the attainable efficiency decreases as the diameter ratio increases. The quantity coefficient curves σ recorded in figure 14 likewise relate only to the experimental blower; that is, they should not be made the basis of the design of any desired compressor; a larger or smaller blower efficiency may also be reached with other quantity coefficients, depending upon the structural dimensions.

In figure 15 are shown the results of a similar consideration, the dependence of the optimum efficiency upon the quantity coefficient at various diameter ratios υ, whereby the expression

$$\sigma_\upsilon = \sigma(1 - \upsilon^2)^2 \qquad (4)$$

proved to be convenient as the basic quantity coefficient. This basic quantity coefficient is therefore the quantity coefficient in the unobstructed tubular section, in contrast to the effective quantity coefficient, which is related to the blower cross section reduced by the hub.

The behavior of axial compressors with variation of their blade settings is also often worth knowing for regulatory problems. In figures 16 to 18 are shown the quantity coefficient as a function of the specific rotary speed K_n for various diameter ratios from 0.75 to 0.95 and the blower efficiency obtained is in each case recorded as a parameter; figure 16 shows the relationships for the calculation setting ($\beta_s = 30^\circ$), figure 17 for the blade turned to another position ($\beta_s = 36^\circ$), and figure 18 for a blade setting ($\beta_s = 24^\circ$) with the blades locked.

The influence of the diameter ratio on the highest pressure coefficient attainable in the case under consideration was also to be clarified within the scope of the investigations. In figure 19 is shown the maximum pressure coefficient ψ_{max} for various blade setting $\beta_s = 18^\circ$ up to $\beta_s = 54^\circ$ as a function of the diameter ratio υ of the experimental blower. If we go on to compare the maximum pressure coefficients obtained for each of various quantity coefficients σ we then obtain the curve of maximum pressure coefficients ψ_{max} shown in figure 20 for various diameter ratios (index $\upsilon = x$) relative to the maximum pressure coefficient for the diameter ratio $\upsilon = 0.755$ $\left(\psi_{max_{\upsilon=0.75}}\right)$. The results show that the relative values of the ratio $\frac{\psi_\upsilon}{\psi_{0.75}}$ depend but little upon the blade setting and quantity coefficient. The mean value curve drawn as a solid line in figure 20 satisfies the equation

$$\frac{\psi}{\psi_{\upsilon=0.75}} = -5.77\upsilon^2 + 7.95\upsilon - 1.71 \qquad (5)$$

The values of the ratio $\frac{\varphi_{max_{\upsilon=x}}}{\varphi_{max_{\upsilon=0.75}}}$ were considered in the same way, and the results are shown in figure 21. In this case also the

sensitivity with respect to blade setting and quantity coefficient is only slight; the formation of the mean values in the latter case satisfies the equation

$$\frac{\varphi}{\varphi_{v=0.75}} = -3.73v^2 + 5.32v - 0.9 \qquad (6)$$

(b) Subdivision of the Total Efficiency, and the Relation Between the Partial Efficiencies and the Diameter Ratio

The power N_{total} required by an axial compressor is larger, by the amount of the losses, than the effective power applied to medium delivered. The losses are composed of the mechanical losses, the windage losses, the gap or clearance losses, and the frictional losses in the blades of the rotor and stator or guiding devices. The energy balance is shown qualitatively in figure 22 in the form of a Sankey diagram, and the condition change during flow through the compressor is shown qualitatively in figure 23 by the Mollier i-s diagram for air (enthalpy-entropy), taking into account the partial losses.

The mechanical losses that occur in the bearings, intermediate packings or seals, and in the joints of the jointed shaft (fig. 24) are comprised in the mechanical efficiency.

$$\eta_{mech} = \frac{N_i}{N_{total}} = \frac{N_{total} - N_m}{N_{total}} = 1 - \frac{N_m}{N_{total}} \qquad (7)$$

In this

N_{total} shaft power (PS)

N_m power for covering the mechanical losses (PS)

N_i internal (indicated) power (PS)

(PS × 0.986318 = HP)

The mechanical efficiency is given the experimental value

$$\eta_{mech} = 0.98$$

The windage losses are produced by air carried along at the ends of the rotating rotor through friction, this air being thrown outward by centrifugal force, whereby eddies are produced. They are taken into account through the windage efficiency. With the symbols in figures 23 and 24 we obtain

$$\eta_{vent} = 1 - \frac{N_{vent}}{N_i} = 1 - \frac{H_{vent}}{H_{th}} = \frac{H_{th} - H_{vent}}{H_{th}} = \frac{H_{st}}{H_{th}} \tag{8}$$

Corresponding to the windage power-loss coefficient

$$k_\lambda = \frac{N}{\frac{\rho}{2} u_a^3 \frac{\pi D^2}{4}}$$

usual in steam turbine practice, the windage power loss, relative to the compressor outer diameter $\left(\frac{d}{D} = \frac{u_i}{u_a} = \upsilon\right)^2$ may be written

$$N_{vent} = k_{\lambda_{vent}} \frac{\rho}{2} \pi r_i^2 u_i^3 = k_{\lambda_{vent}} \frac{\rho}{2} \pi R^2 u_a^3 \upsilon^5 \tag{9}$$

According to A. Stodola[3]

$$k_{\lambda_{vent}} = 0.0021 \text{ to } 0.0028$$

in a steam turbine for a smooth rotor and in a not too narrow axial gap at a comparable Reynolds number. For the test blower with the very great axial gap but with somewhat greater roughness $k_{\lambda_{vent}}$ should be about the same magnitude. The greater roughness builds up a greater stagnation layer and thus in effect cuts down the clearance and consequent windage loss. In evaluating the test therefore, the assumption was made that $k_{\lambda_{vent}} = 0.0028$.

---

[2]The shaft diameter is assumed to be small. When the mass density is different on the two sides of the rotor, its mean value is to be inserted.

[3]Stodola, A.: Dampf- und Gasturbinen. 6. Aufl. Berlin. J. Springer 1924.

If for the internal power of the blower we write:

$$N_i = k_{l_i} \frac{\rho}{2} \pi R^2 u_a^3 \tag{10}$$

whereby, using equation (15) for the internal adiabatic efficiency, the power coefficient is

$$k_{l_i} = \frac{\varphi\psi}{\eta_{i_{ad}}} (1 - v^2) \tag{11}$$

then with

$$\eta_{total} = \eta_{i_{ad}} \eta_{mech}$$

$$\eta_{vent} = 1 - \frac{k_{l_{vent}} \eta_{i_{ad}}}{\varphi\psi} \frac{v^5}{1 - v^2} = 1 - \frac{k_{l_{vent}} \eta_{total}}{\varphi\psi \eta_{mech}} \frac{v^5}{1 - v^2} \tag{12}$$

The gap or clearance losses occur as a result of the gap or clearance necessary for operational reasons between the rotor and housing $\left(N_{vol_R} \right)$ and under certain circumstances between the stator or bearing and shaft $\left(N_{vol_L} \right)$. Because of the pressure drop that exists between the pressure side and the suction side, a portion of the working medium ΔG_R or ΔG_L flows back in some cases. The clearance losses are taken into account by the volumetric efficiency η_{vol}

$$\eta_{vol} = 1 - \frac{H_{vol}}{H_{st}} \tag{13}$$

The total volumetric head loss

$$H_{vol} = H_{vol_R} + H_{vol_L}$$

is hereby composed of the volumetric head losses in the rotor gap $\left(H_{vol_R}\right)$ and in the stator gap $\left(H_{vol_L}\right)$. By the volumetric efficiency of the rotor and of the stator are understood

$$\eta_{vol_R} = \frac{\dot{G}}{\dot{G} + \Delta\dot{G}_R}$$

$$\eta_{vol_L} = \frac{\dot{G}}{\dot{G} + \Delta\dot{G}_L}$$

Let them be regarded in the following as given. With them we get

$$H_{vol_R} = \left(1 - \eta_{vol_R}\right)H_{id_{stR}}$$

$$H_{vol_L} = \left(1 - \eta_{vol_L}\right)H_{id_{stL}}$$

or, if H_u indicates the "ideal" head of the rotor

$$H_u = H_{st} - H_{vol} = \eta_{vol}H_{st}$$

and w indicates the degree of reaction

$$H_{id_{stR}} = wH_u$$

$$H_{id_{stL}} = (1 - w)H_u$$

$$H_{vol_R} = \left(1 - \eta_{vol_R}\right)wH_u$$

$$H_{vol_L} = \left(1 - \eta_{vol_L}\right)(1 - w)H_u$$

and consequently

$$\eta_{vol} = 1 - \eta_{vol}\left[\left(1 - \eta_{vol_R}\right)w + \left(1 - \eta_{vol_L}\right)(1 - w)\right]$$

or

$$\eta_{vol} = \frac{1}{2 - \eta_{vol_R} w - \eta_{vol_L}(1 - w)}$$

for

w approaching 1; η_{vol_R} approaching 1; η_{vol_L} approaching 1,

we obtain as a first approximation

$$\eta_{vol} \text{ approaches } \eta_{vol_R}$$

The approximation is particularly applicable to rotors having a following stator.

The frictional losses $H_{(R+L)_{loss}}$ at the blades of the rotor $H_{R_{loss}}$ and the stator $H_{L_{loss}}$ are taken into account through the blade efficiency η_u. This is given as the ratio of the head H_{ad} actually reached to the head H_u (fig. 23) remaining after deduction of the windage $\left(H_{vent}\right)$ and clearance $\left(H_{vol}\right)$ losses from the theoretical head H_{th}:

$$\eta_u = \frac{H_{ad}}{H_u} = \frac{H_{th} - H_{vent} - H_{vol} - H_{(R+L)_{loss}}}{H_{th} - H_{vent} - H_{vol}} \qquad (14)$$

From the foregoing definitions we consequently obtain for the internal efficiency, that is, the ratio of the useful power to the total power transmitted to the working medium

$$\eta_i = \eta_{i_{ad}}$$

$$= \frac{H_{ad}}{H_{th}}$$

$$= \frac{H_{th} - H_{vent}}{H_{th}} \frac{H_{th} - H_{vent} - H_{vol}}{H_{th} - H_{vent}} \frac{H_{th} - H_{vent} - H_{vol} - H_{(R+L)_{loss}}}{H_{th} - H_{vent} - H_{vol}}$$

$$= \frac{H_{st}}{H_{th}} \frac{H_u}{H_{st}} \frac{H_{ad}}{H_u}$$

$$= \eta_{vent}\eta_{vol}\eta_u \qquad (15)$$

The product $\eta_{vol}\eta_u = \frac{H_{ad}}{H_{st}}$ may be termed the stage efficiency η_{st}.

For the total or adiabatic efficiency we consequently obtain

$$\eta_{ad} = \eta_{total} = \eta_{i_{ad}}\eta_{mech} = \eta_{vent}\eta_{vol}\eta_u\eta_{mech} \qquad (16)$$

In accordance with this we obtain for the separate powers (mkg/s) the following relationships:

Total drive power $N_{total} = N_i + N_{mech}$

Internal power $N_i = H_{th}\dot{G} = \eta_{mech}N_{total}$

Stage power $N_{st} = H_{st}\dot{G} = \left(H_{th} - H_{vent}\right)\dot{G} = \eta_{vent}N_i$

Blade power $N_u = H_u\dot{G} = \left(H_{th} - H_{vent} - H_{vol}\right)\dot{G} = \eta_{vol}N_{st}$

Useful power $N_n = H_{ad}\dot{G} = \left[H_{th} - H_{vent} - H_{vol} - H_{(R+L)_{loss}}\right]\dot{G} = \eta_u N_u$.

Windage loss power $N_{vent} = H_{vent}\dot{G}$

Clearance loss power $N_{vol} = H_{vol}\dot{G}$

Blade loss power $N_{(R+L)_{loss}} = H_{(R+L)_{loss}}G$

The qualitative relationship between the diameter ratio υ and the blade efficiency η_u may be derived from the following considerations.

The blade efficiency of an axial blower in terms of one blade element at a distance r from the axis is

$$\eta_R' = \frac{1 - \epsilon_R \varphi'_{\infty_R}}{1 + \frac{\epsilon_R}{\varphi'_{\infty_R}}}$$

and

$$\eta_L' = \frac{1 - \epsilon_L \varphi'_{\infty_L}}{1 + \frac{\epsilon_L}{\varphi'_{\infty_L}}} \qquad (17)$$

The index (') hereby indicates that the magnitudes relate only to one blade element. The effective capacity coefficient is hereby

$$\varphi'_{\infty_R} = \frac{c_m}{u' - \frac{c'_u}{2}}$$

$$\varphi'_{\infty_L} = \frac{c_m}{\frac{c'_u}{2}}$$

and because

$$\frac{c_m}{u'} = \varphi'$$

and

$$c_u' = \frac{gH_u}{u} = u\,\frac{\psi_u}{2} = u\,\frac{\psi}{2\eta_u}$$

$$\frac{c_u'}{u'} = \frac{\psi'}{2\eta_u'}$$

Consequently, for the rotor

$$\varphi'_{\infty_R} = \frac{\varphi'}{1 - \frac{\psi'}{4\eta_u'}}$$

and for the stator

$$\varphi'_{\infty_L} = \frac{\varphi'}{\frac{\psi'}{4\eta_u'}}$$

Furthermore with a negligible change in density, with

$$\Delta p = \gamma H_{ad}$$

$$\Delta p_u = \gamma H_u$$

$$\Delta p_u = \frac{\rho}{2}\,u^2\,\frac{\psi}{\eta_u} = \frac{\rho}{2}\,u'^2\,\frac{\psi'}{\eta_u'} = \Delta p_{R_{id,st}} + \Delta p_{L_{id,st}}$$

and the ideal static pressure rise in the stator (index L)

$$\Delta p_{L_{id,st}} = \frac{\rho}{2} c_u{}'^2 = \frac{\rho}{2} u'^2 \left(\frac{c_u'}{u'}\right)^2 = \frac{\rho}{2} u'^2 \left(\frac{\psi'}{2\eta_u'}\right)^2$$

and in the rotor (index R)

$$\Delta p_{R_{id,st}} = \frac{\rho}{2} u'^2 \frac{\psi'}{\eta_u'} - \frac{\rho}{2} u'^2 \left(\frac{\psi'}{2\eta_u'}\right)^2 = \frac{\rho}{2} u'^2 \left[\frac{\psi'}{\eta_u'} - \left(\frac{\psi'}{2\eta_u'}\right)^2\right]$$

Consequently for the blower element

$$\Delta p = \Delta p_u = \Delta p_{(R+L)_{loss}}$$

whereby

$$\Delta p_{(R+L)_{loss}} = \Delta p_{R_{loss}} + \Delta p_{L_{loss}}$$

and the pressure loss in the rotor

$$\Delta p_{R_{loss}} = \left(1 - \eta_R'\right)\left[\frac{\psi'}{\eta_u'} - \left(\frac{\psi'}{2\eta_u'}\right)^2\right] \frac{\rho}{2} u'^2$$

and the pressure loss in the stator

$$\Delta p_{L_{loss}} = \left(1 - \eta_L'\right)\left(\frac{\psi'}{2\eta_u'}\right)^2 \frac{\rho}{2} u'^2$$

So long as $\frac{\psi'}{2\eta_u'} \ll 1$[4], we may however write as an estimate for each element of the blower

$$\Delta p_{L_{loss}} \approx 0$$

that is

$$\Delta p_{R_{loss}} \approx \Delta p_{(R+L)_{loss}}$$

Furthermore if we write

$$\varphi'_{\infty_R} \approx \varphi'$$

then

$$\eta_u' \approx \eta_R' = \frac{1 - \epsilon_R \varphi'}{1 + \frac{\epsilon_R}{\varphi'}}$$

Assuming a constant mean flow velocity (c_m = constant) and a constant profile drag-lift ratio (ϵ_R) independent of the blade section r under consideration, we obtain for the entire blower, with the relationship $\varphi' = \frac{\varphi}{x}$ whereby $x = \frac{r'}{R}$

$$\eta_u = \frac{\int_{r_i}^{R} \eta_u' 2r\pi \, dr}{\int_{r_i}^{R} 2r\pi \, dr} = \frac{2\varphi}{\epsilon_R(1 + \upsilon)} - \frac{2\varphi^2\left(1 + \frac{1}{\epsilon_R^2}\right)}{1 - \upsilon^2} \ln \frac{1 + \frac{\varphi}{\epsilon_R}}{\upsilon + \frac{\varphi}{\epsilon_R}} \qquad (18)$$

---

[4]Translator's note: $\ll$ means is much less than.

Evaluation of equation (18) is very tiresome, particularly for large values of the capacity coefficient φ. However, so long as $\epsilon_R \ll \varphi'$ then

$$\eta_u' \approx \eta_R' \approx (1 - \epsilon_R\varphi')\left(1 - \frac{\epsilon_R}{\varphi'}\right) = 1 - \epsilon_R\left(\varphi' + \frac{1}{\varphi'}\right)$$

and

$$\eta_u = \frac{\int_{r_i}^{R} \eta_u' 2r\pi \, dr}{\int_{r_i}^{R} 2r\pi \, dr} = 1 - \epsilon_R\left(\frac{2\varphi}{1 + \upsilon} + \frac{2}{3\varphi}\,\frac{1 + \upsilon + \upsilon^2}{1 + \upsilon}\right) \tag{19}$$

Through the similar equation, which however takes into account the asymptotic behavior for small values of φ

$$\eta_u = \frac{1 - \frac{2}{1 + \upsilon}\epsilon_R\varphi}{1 + \frac{2}{3}\,\frac{1 + \upsilon + \upsilon^2}{1 + \upsilon}\,\frac{\epsilon_R}{\varphi}} \tag{19a}$$

exact results are quite closely approximated both for large as well as for small values of φ. Evaluation of equation (19a) is shown in figure 25.

Taking the clearance losses into account the internal adiabatic efficiency becomes

$$\eta_{i_{ad}} = \eta_{vent}\eta_{vol}\eta_u$$

and the over-all efficiency at the blower coupling becomes

$$\eta_{total} = \eta_{ad} = \eta_{vent}\eta_{vol}\eta_u\eta_{mech} \tag{20}$$

Consequently,

$$\eta_u = \frac{\eta_{total}}{\eta_{vent}\eta_{vol}\eta_{mech}} = \frac{\eta_{total}}{\eta_{vol}\eta_{mech}} \frac{1}{1 - \frac{k_{\zeta_{vent}}\eta_{total}}{\varphi\psi\eta_{mech}} \frac{v^5}{1 - v^2}} \tag{21}$$

With the values $\eta_{vol} = 0.98$, $\eta_{mech} = 0.98$ based upon test results and the assumed value $k_{\zeta_{vent}} = 0.0028$ we obtain the values shown in table I for the blade efficiency and the corresponding effective drag-lift ratios according to figure 25, in each case for the experimentally found optimum value.

TABLE I

PERIPHERAL EFFICIENCY η_u AND GRID DRAG-LIFT RATIO ϵ_R FOR VARIOUS DIAMETER RATIOS v

v	ψ	φ_R	η_{total}	η_u	ϵ_R
0.75	0.730	0.470	0.778	0.813	0.0838
.80	.710	.440	.748	.783	.093
.85	.665	.406	.705	.742	.103
.90	.590	.352	.648	.674	.117
.95	.465	.300	.515	.562	.140

(c) The Influence of the Diameter Ratio on the Drag-Lift Ratio

The drag-lift ratio ϵ_R of the rotor or stator is evidently considerably greater than the drag-lift ratio ϵ_p we might expect for the profile itself. The difference is evidently caused by the fact that not only the blades themselves but also the portion of the hub surface and housing surface lying between the blades cause flow losses. These surfaces, at least with a sufficiently large number of blades, that is, sufficiently close spacing, are under substantially the same flow conditions, that is, the same acceleration and retardation, as the profiles along their axial extension. Therefore, the flow losses hereby produced stand in approximately the same ratio

to the flow losses at the profile surfaces as these portions of the hub surfaces $F_i = zt_i l_i \sin \beta_i$ and housing surfaces $F_a = zt_a l_a \sin \beta_a$ stand to the profile surfaces $F_p = 2zl_m(R - \eta)$. Consequently, the ratio of the drag coefficient c_{w_r} which is determinative for the efficiency η_R to the drag coefficient c_{w_p} of the profile in a smooth grid flow, and consequently also the ratio of the corresponding drag-lift ratios becomes

$$\frac{c_{w_r}}{c_{w_p}} = \frac{\epsilon_R}{\epsilon_P} = 1 + \frac{t_a l_a \sin \beta_a + t_i l_i \sin \beta_i}{2l_m(R - \eta)} \approx 1 + \frac{t_m \sin \beta_m}{R - r_i} \qquad (22)$$

In this

$$t_m = \frac{t_a l_a \sin \beta_a + t_i l_i \sin \beta_i}{2(l_a \sin \beta_a + l_i \sin \beta_i)} \approx \frac{2\pi r_m}{z} = \frac{\pi}{z}(R + r_i)$$

$$l_m = \frac{l_a \sin \beta_a + l_i \sin \beta_i}{2(\sin \beta_a + \sin \beta_i)} \approx \frac{l_a + l_i}{2}$$

$$\sin \beta_m = \frac{\sin \beta_a + \sin \beta_i}{2}$$

$$\beta_m \approx \frac{\beta_a + \beta_i}{2}$$

Consequently,

$$\epsilon_R = \epsilon_P \left(1 + \frac{\pi}{z} \frac{1 + \upsilon}{1 - \upsilon} \sin \beta_m\right) = \epsilon_P k_\epsilon \qquad (23)$$

The values compiled in table II were found with the foregoing test results for the test blower $z = 48$ blades.

TABLE II

PROFILE DRAG-LIFT RATIOS ϵ_p OF THE TEST BLOWER FOR VARIOUS DIAMETER RATIOS υ

υ	β_m (deg)	$\sin \beta_m$	$\frac{\pi}{z} \frac{1+\upsilon}{1-\upsilon}$	k_ϵ	$\epsilon_p = \frac{\epsilon_R}{k_\epsilon}$
0.75	48	0.743	0.458	1.341	0.0618
.80	47	.731	.589	1.431	.0650
.85	44	.695	.818	1.568	.0657
.90	39	.621	1.242	1.782	.0656
.95	32	.530	2.582	2.369	.0590

The evaluation of the test results can also be effected graphically when k_ϵ has been computed, as is shown in figure 25.

For many applications it has been found advantageous to introduce

$$\frac{t_a + t_i}{2} = t_m = \frac{t_i}{2} \frac{1+\upsilon}{\upsilon}$$

$$\frac{l_a \sin \beta_a + l_i \sin \beta_i}{2} = \frac{l_a \frac{\sin \beta_a}{\sin \beta_i} + l_i}{2} \sin \beta_i \approx l_m \sin \beta_i$$

$$\frac{t_i}{2R} = \frac{t_i}{D_a} = \tau'$$

and thus to write

$$\epsilon_R = \epsilon_p \left(1 + \frac{\tau'}{\upsilon} \frac{1+\upsilon}{1-\upsilon}\right) = \epsilon_p k_\epsilon$$

In order to evaluate these drag-lift ratios, let us first make an estimate of the corresponding mean angle of incidence α_m the mean circulation coefficient c_{Γ_m} or the mean lift coefficient c_{a_m} and the mean profile-drag coefficient $c_{w_{p_m}}$ by means of (See fig. 26.)

$$\left.\begin{aligned} \alpha_m &= \beta_m - \sigma_{\infty_m} = \beta_m - \operatorname{arc\,tan} \frac{c_m}{u - \frac{\Delta w_u}{2}} = \beta_m - \operatorname{arc\,tan} \frac{\varphi_{R_m}}{1 - \frac{\psi_m}{4\eta_u}} \\ c_{\Gamma_m} &= 2 \frac{t}{l} \frac{w_{u_2} - w_{u_1}}{w_\infty} = 2\left(\frac{t}{l}\right)_m \frac{\frac{\psi_m}{2\eta_u}}{\sqrt{\varphi_m^2 + \left(1 - \frac{\psi_m}{4\eta_u}\right)^2}} \end{aligned}\right\} \quad (24)$$

Hereby

$$\varphi_{R_m} = \frac{2}{1 + v} \varphi_R$$

$$\psi_m = \left(\frac{2}{1 + v}\right)^2 \psi$$

$$t_m = \frac{\pi}{z} (1 + v) R$$

Furthermore

$$c_{a_m} = c_\Gamma \frac{\eta_u + \tan^2 \sigma_\infty}{1 + \tan^2 \sigma_\infty}$$

$$c_{w_{p_m}} = \epsilon\, c_{a_m}$$

For the present test results we then obtain the following values for c_{Γ_m}, c_{a_m}, $c_{w_{p_m}}$ shown in table III.

TABLE III

ν	t_m	l_m	(t/l)	φ_{R_m}	ψ_m	η_u	σ_{∞_m} (deg)	α (deg)	c_{Γ_m}	ϵ_p	c_{a_m}	$c_{w_{p_m}}$
0.75	0.0257	0.0312	0.826	0.537	0.955	0.813	37.8	10.2	1.15	0.0618	1.015	0.0628
.80	.0264	.0312	.850	.489	.878	.783	34.6	12.4	1.16	.0650	.989	.0643
.85	.0272	.0312	.878	.432	.778	.742	30.7	13.3	1.12	.0657	.907	.0596
.90	.0279	.0312	.897	.371	.653	.674	26.3	12.7	1.18	.0656	.87	.057
.95	.0257	.0312	.921	.308	.491	.562	21.8	10.2	1.01	.0590	.629	.0371
1.00	.0294	.0312	.945	---	---	---	----	----	----	----	---	----

Because the blade efficiency η_u increases with the flow coefficient for the diameter ratios investigated and for a constant ϵ_R and therefore with a fixed blade setting for a constant ϵ_p also, the operating point with the optimum ϵ_p evidently lies at a lower φ than the operating point with η_{opt}. The values ϵ_R and ϵ_p obtained from the above experimental values at the optimum efficiency η_{opt} must therefore be somewhat worse, larger that is, than the optimum value possible. With this optimum value of ϵ_R or ϵ_p is also associated a lift coefficient that is somewhat larger, but which must in turn be somewhat smaller than the maximum attainable lift coefficient

$$c_{a_{max}} > c_{a_{\epsilon_{opt}}} > c_{a_{\eta_{opt}}}$$

Evaluation of the tests shows that $\epsilon_{p_{\eta_{opt}}}$ and $c_{a_{\eta_{opt}}}$, respectively, are, within the limits of test and evaluation accuracy, independent of the diameter ratio. The decrease in efficiency and in the pressure coefficient with an increase in the diameter ratio is consequently to be ascribed chiefly to the increasing influence of the portions of the hub surface and housing inner surface between the blades, which cause proportionally the same flow losses as the blades themselves, but which however contribute nothing to the useful work.

The efficiency lines shown in the lower part of figures 4 to 8 have in each case an envelope. The points lying upon these envelopes must in each case correspond to an operating condition of optimum drag-lift ratio ϵ_p. If this drag-lift ratio were known, then the envelope could easily be calculated by the aid of the relationships given. Now as a check let $\epsilon_{p_{opt}} = 0.063$ be taken as the basis for all diameter ratios and blade setting.

φ, ψ, and η_{total} are known for each point of the envelope. From this we first obtain the peripheral efficiency in accordance with equation (21) (line η_{u_2} fig. 27). With $\epsilon_R = \epsilon_{p_{opt}}$ we have an upper limit for η_u according to equation (19) which leaves out of account the flow losses at the lateral guides of the flow past the hub and housing in the region of the blades (line η_{u_0} in fig. 27). With $\epsilon_R = k_\epsilon \epsilon_p$ (according to equation (23)) these flow losses are taken into account as respects the peripheral efficiency η_u according to equation (19a) (line η_{u_1} in fig. 27). The results of these evaluations are reproduced in figure 27.

The difference (c) between $\eta_u = \eta_{u_1}$ computed with $\epsilon_p = 0.063$ and the $\eta_u = \eta_{u_2}$ obtained from the test results may be ascribed only to the slightest extent to the factors neglected in deriving equation (19). No substantial change in the profile drag-lift ratio ϵ_p occurs even when there is a change in the blade setting and consequently in the load distribution along the radius.

The main influence is probably the changed flow to the stator. Because this influence is considerable, we contemplate making tests of the entry shock into the stators.

4. SUMMARY

The tests on one single-stage axial blower with a variable diameter ratio gave a decrease in the maximum attainable pressure coefficient as the diameter increased. A comparison of the throttle coefficients for the cases in question led to a similar result. As further evaluation of the tests and further consideration showed, the optimum efficiency attainable is dependent upon the specific rotary speed K_n and the quantity coefficient σ_v related to the unobstructed tubular cross section, but it always decreases as the diameter ratio increases.

In evaluating the tests the over-all efficiency was divided into its partial efficiencies. Because in the test blower, with relatively small drive power but with large structural dimensions, the influence of rotor frictional and windage losses had their effect, the efficiencies attained were low. This should be particularly noted in order to avoid errors. With aircraft-engine axial superchargers, usually of multistage design, the windage losses for example would be practically negligible. The same applies to a jet-engine compressor. Indeed in this case the absolute windage losses are similar to those with the test blower; however, the drive losses are considerably greater, for which reason the windage losses may again be neglected in most cases.

Theoretical considerations, which permit predetermination of the internal adiabatic efficiency, agree very well with the results of the tests. As the diagrams show, the internal adiabatic efficiency, which is decisive for compressor energy considerations, is extraordinarily sensitive to the drag-lift ratio, which indicates the necessity of optimum surface quality and precision manufacture for axial compressors. Moreover the results show that the optimum value of the internal efficiency is dependent upon the flow coefficient and upon the diameter ratio used in the case under consideration. The other partial efficiencies, which determine the coupling power required in the case in question, are to a great extent not influenced by the diameter ratio, and are largely dependent upon the precision of manufacture (η_{vol}), upon the type of drive (η_{mech}), and upon the structural dimensions (η_{vent}), but these are of minor significance in a comparison with the blade efficiency.

Translated by W. G. Weekley
Bureau of Aeronautics,
Navy Department

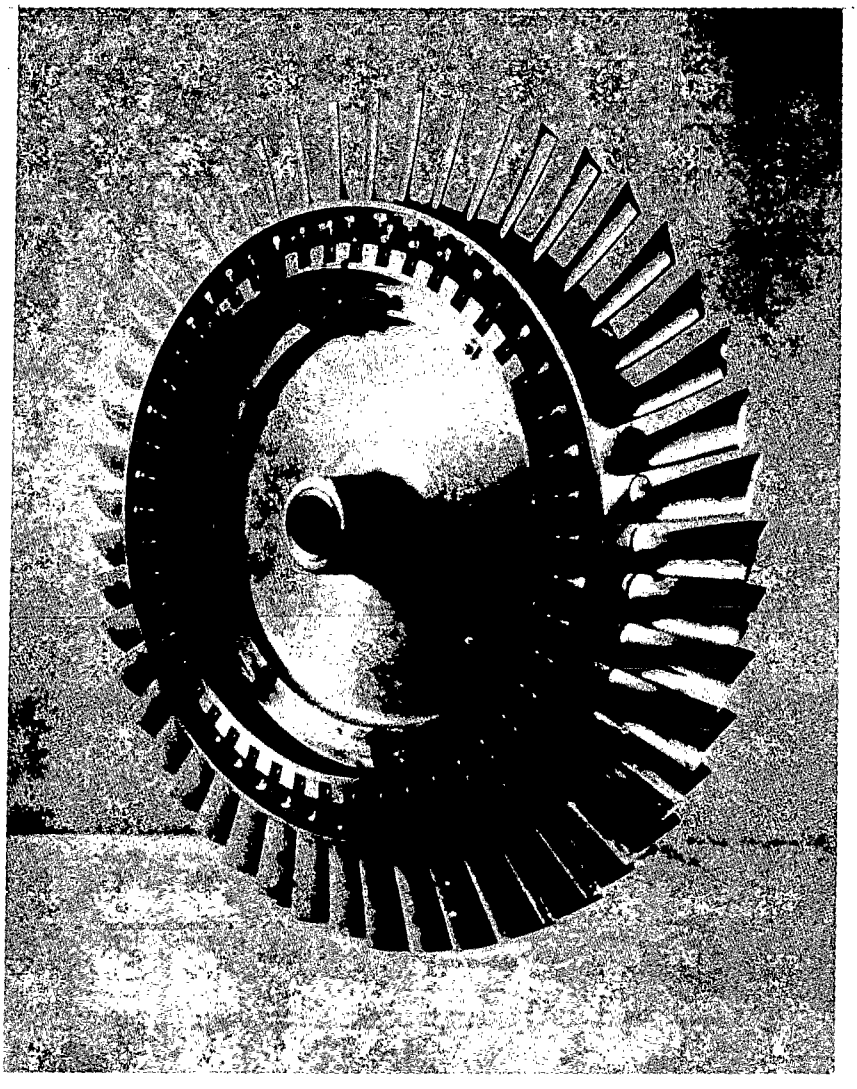

Figure 1.- Rotor of test blower with $z = 48$ blades.

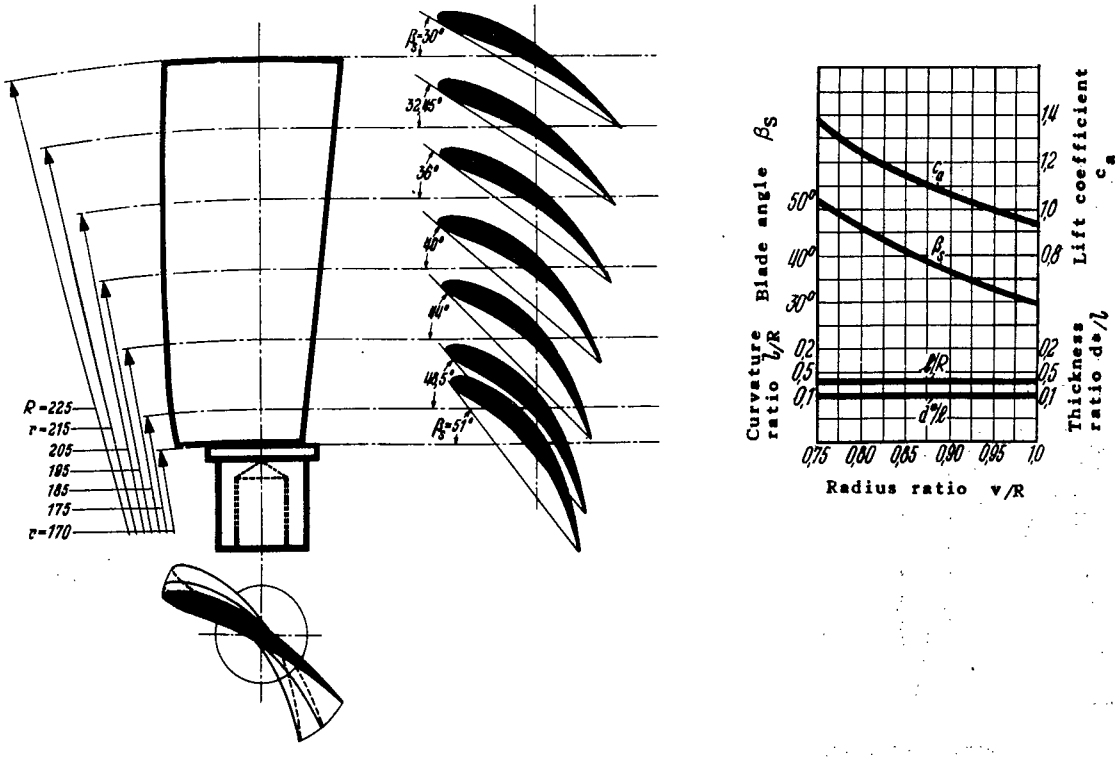

Figure 2.- Blade sections and characteristic dimensions of the rotor.

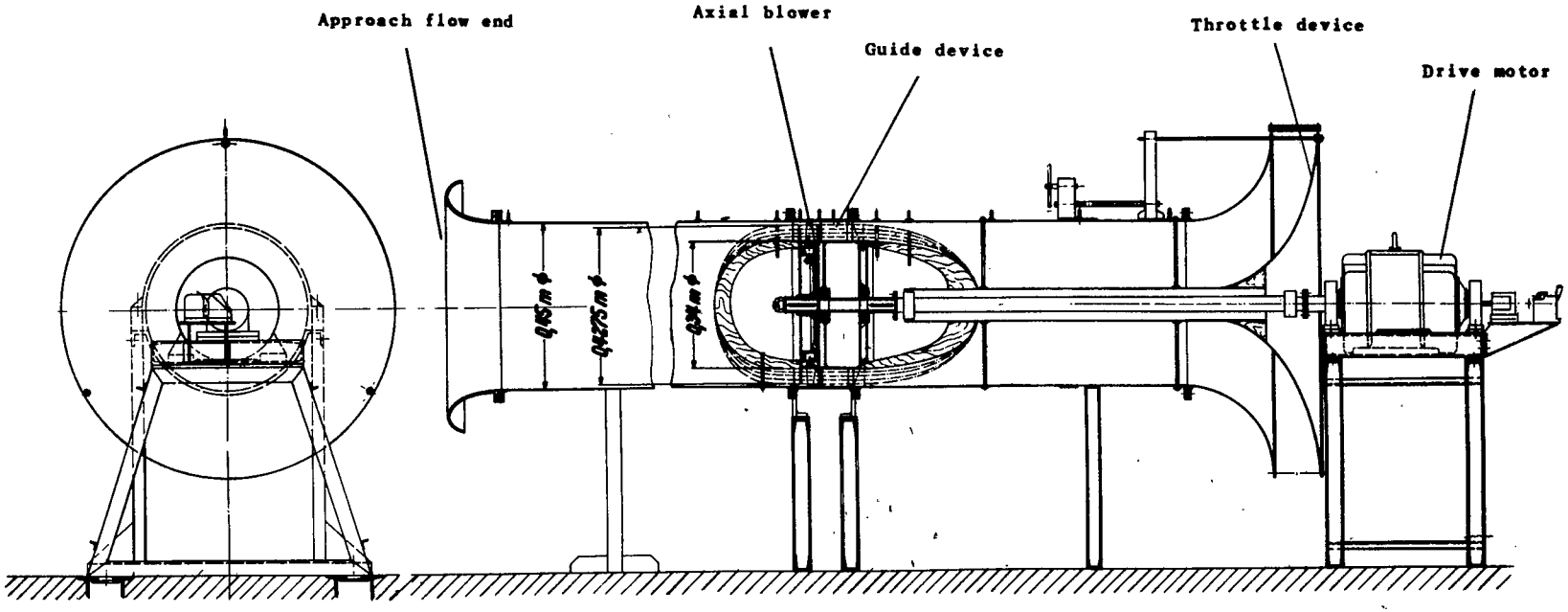

Figure 3.- Test stand for investigating the influence of the diameter ratio.

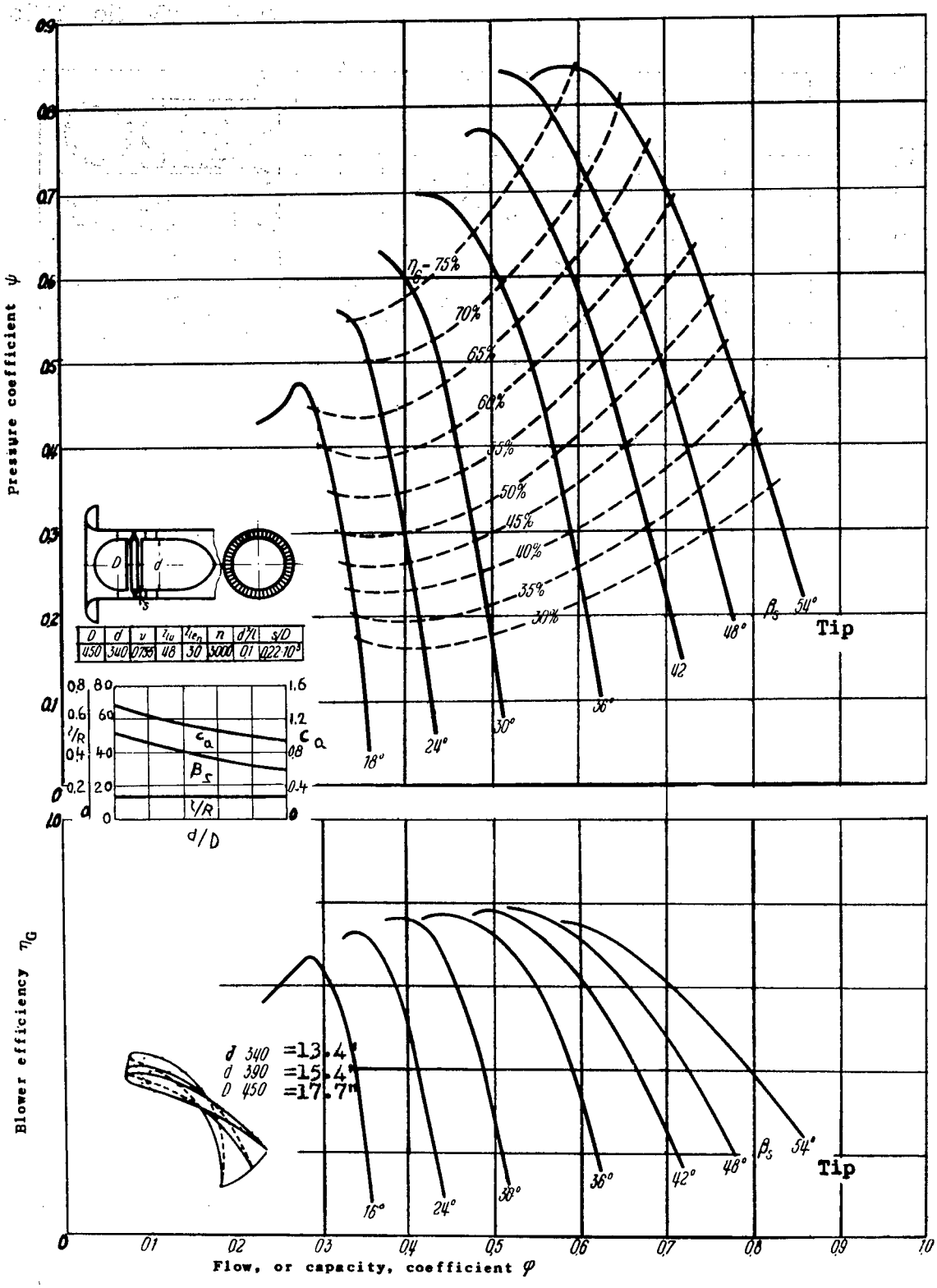

Figure 4.- Characteristics diagram for the test blower with a diameter ratio $\upsilon = 0.755$. Blade angle.

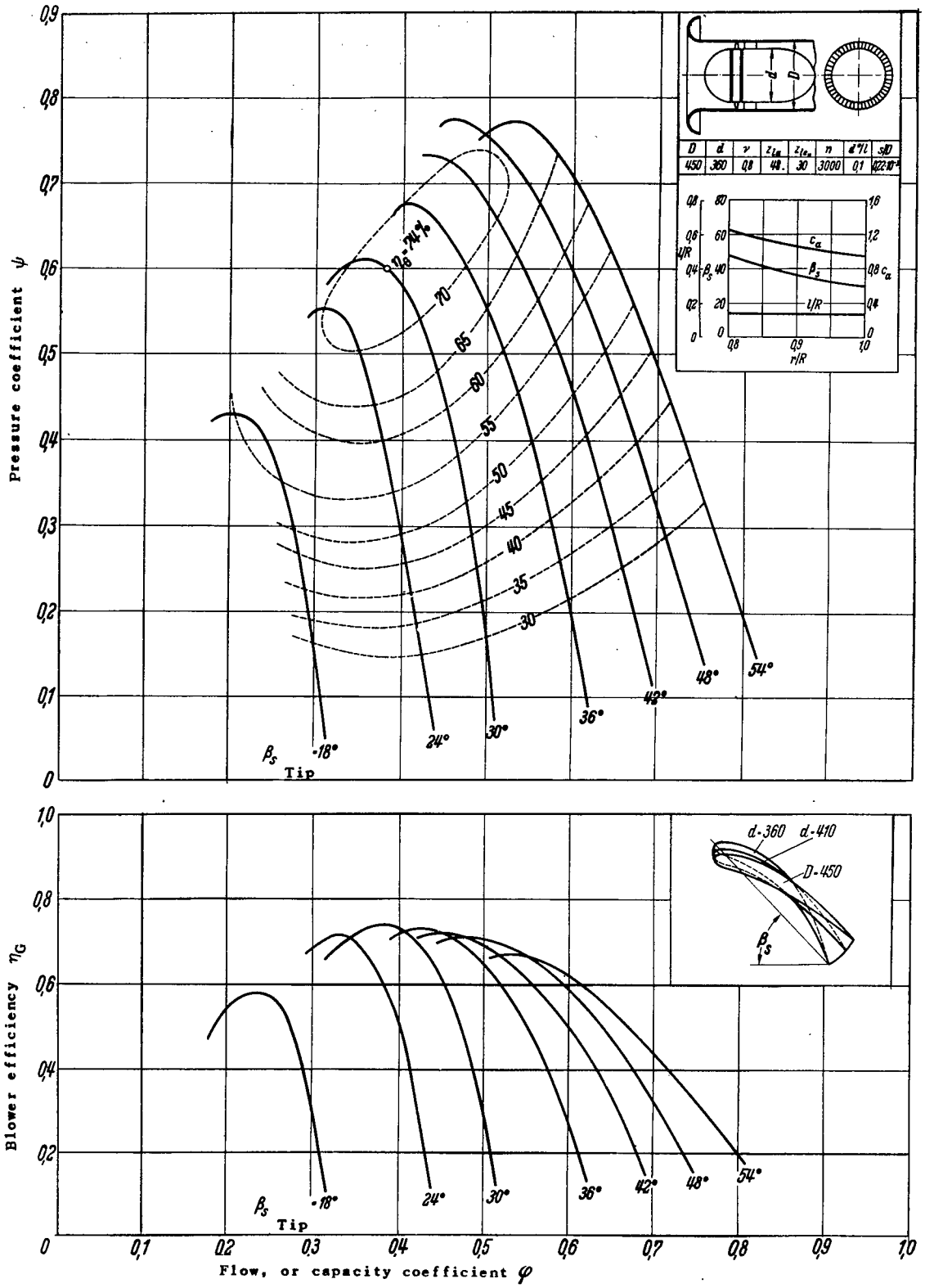

Figure 5.- Characteristics diagram for the test blower with a diameter ratio $\upsilon = 0.80$.

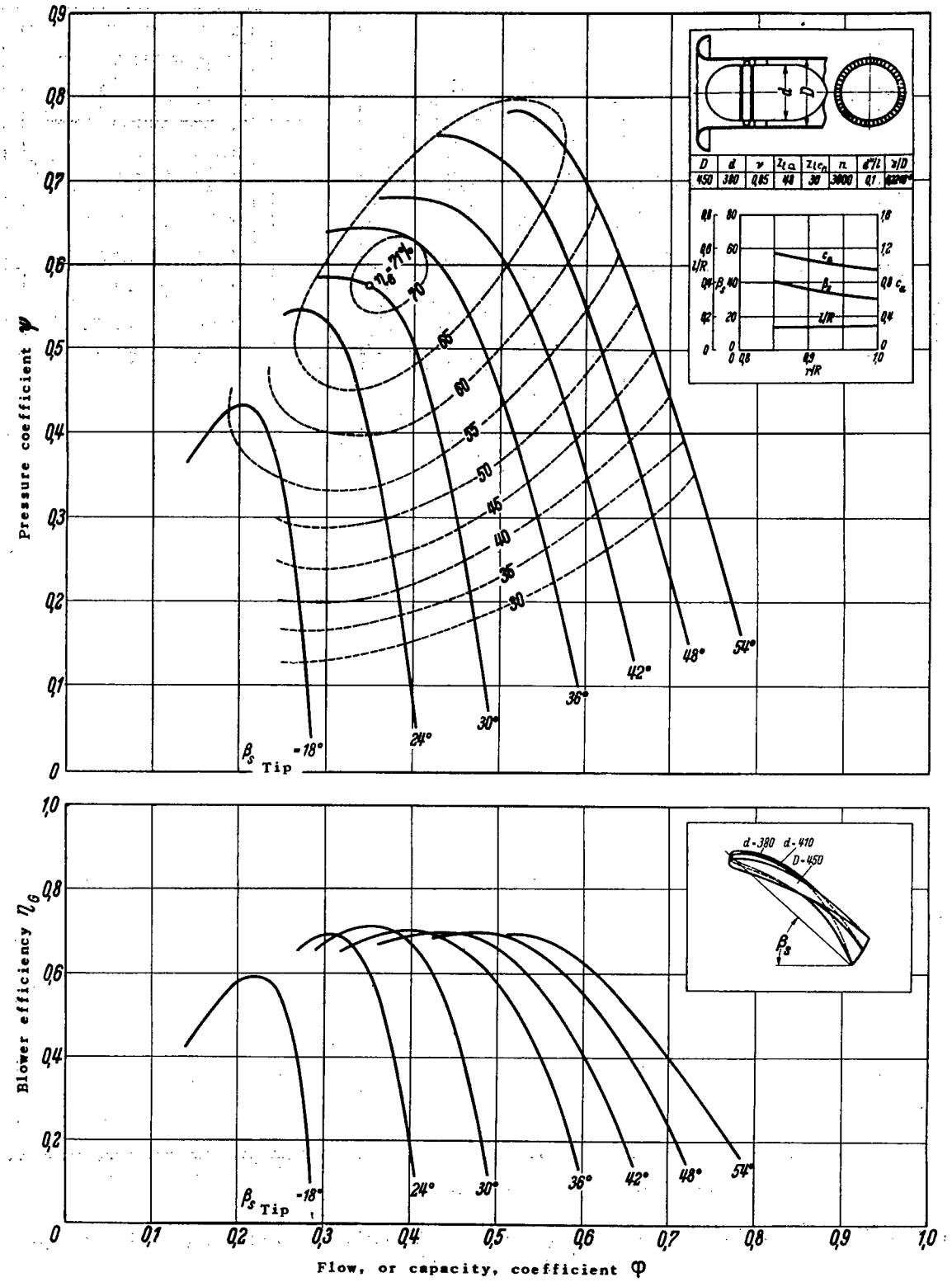

Figure 6.- Characteristics diagram of the test blower with a diameter ratio $\upsilon = 0.85$.

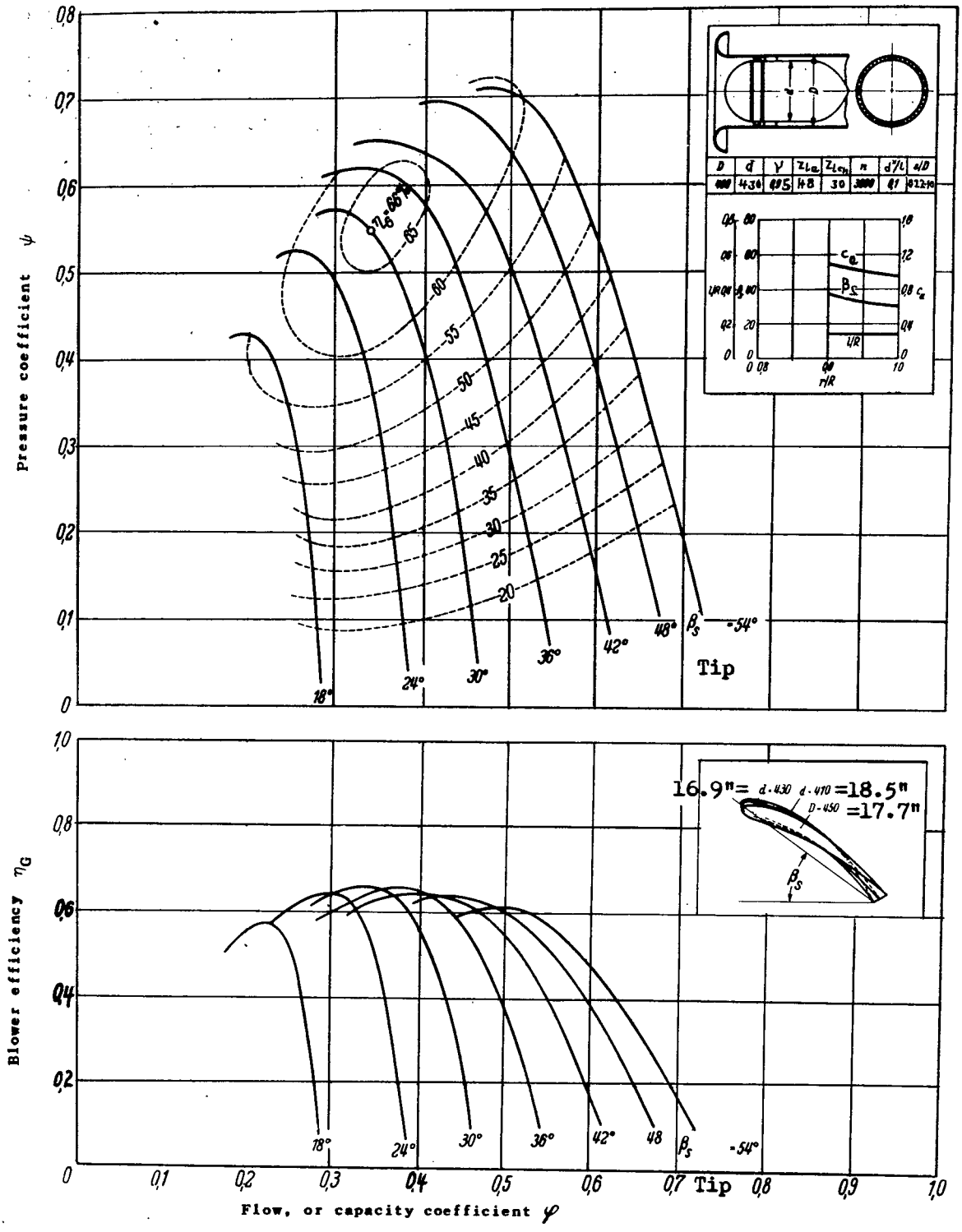

Figure 7.- Characteristics diagram of the test blower with a diameter ratio $\upsilon = 0.90$.

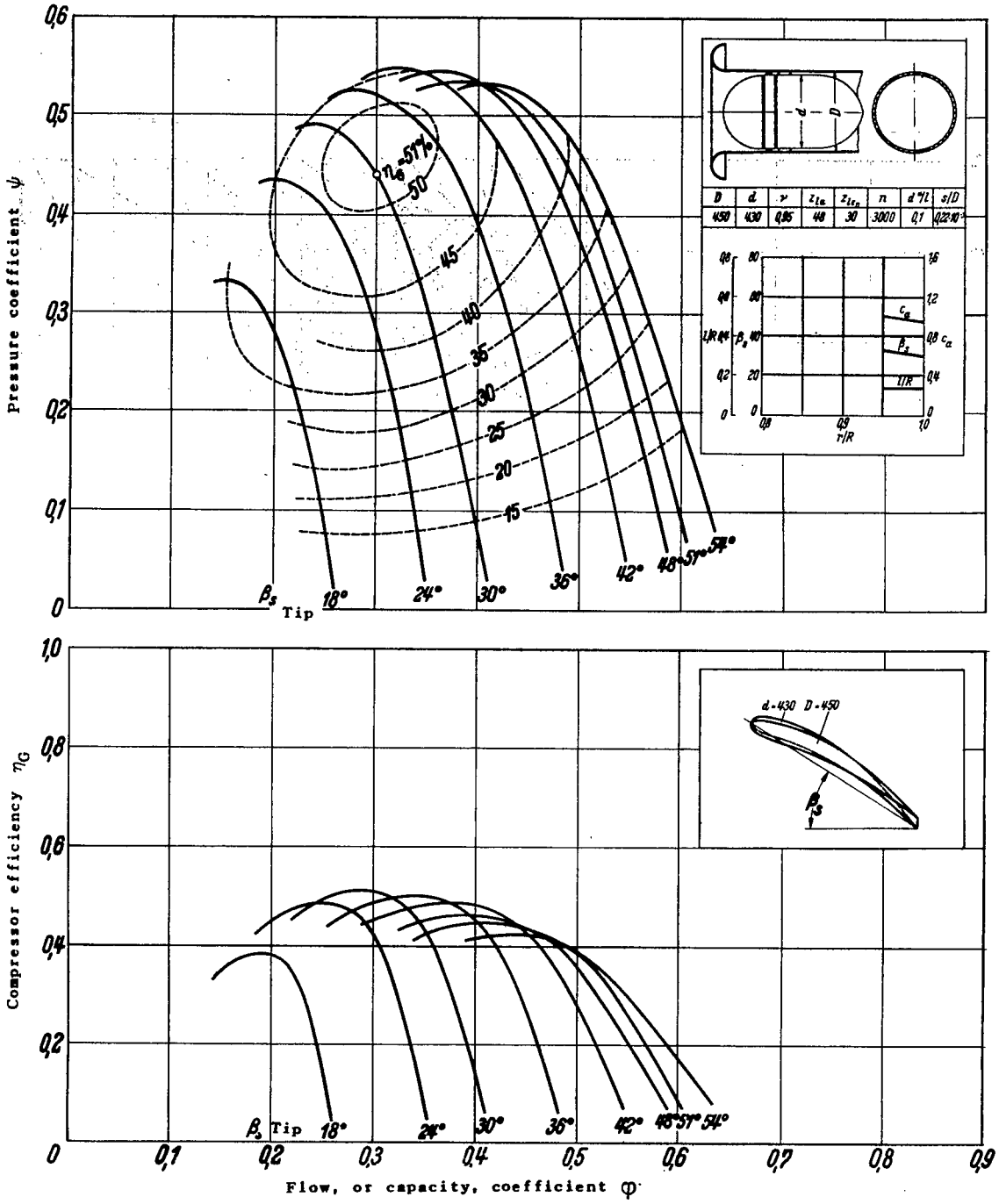

Figure 8.- Characteristics curves of the test compressor with a diameter ratio $\upsilon = 0.95$.

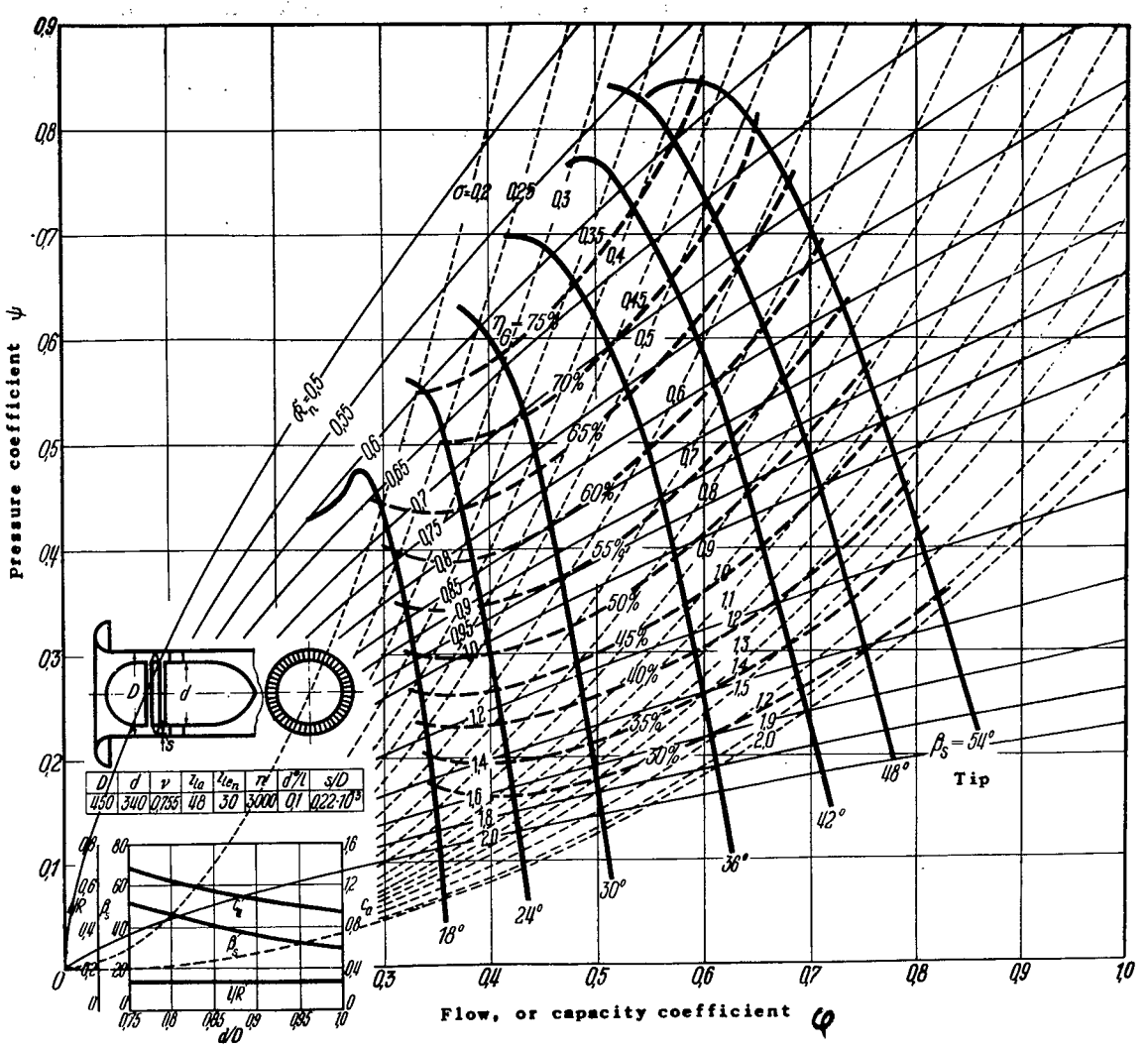

Figure 9.- Characteristics diagram of the test blower with lines of constant specific rotary speed K_n and constant throttling or quantity coefficients σ. Diameter ratio $\upsilon = 0.755$.

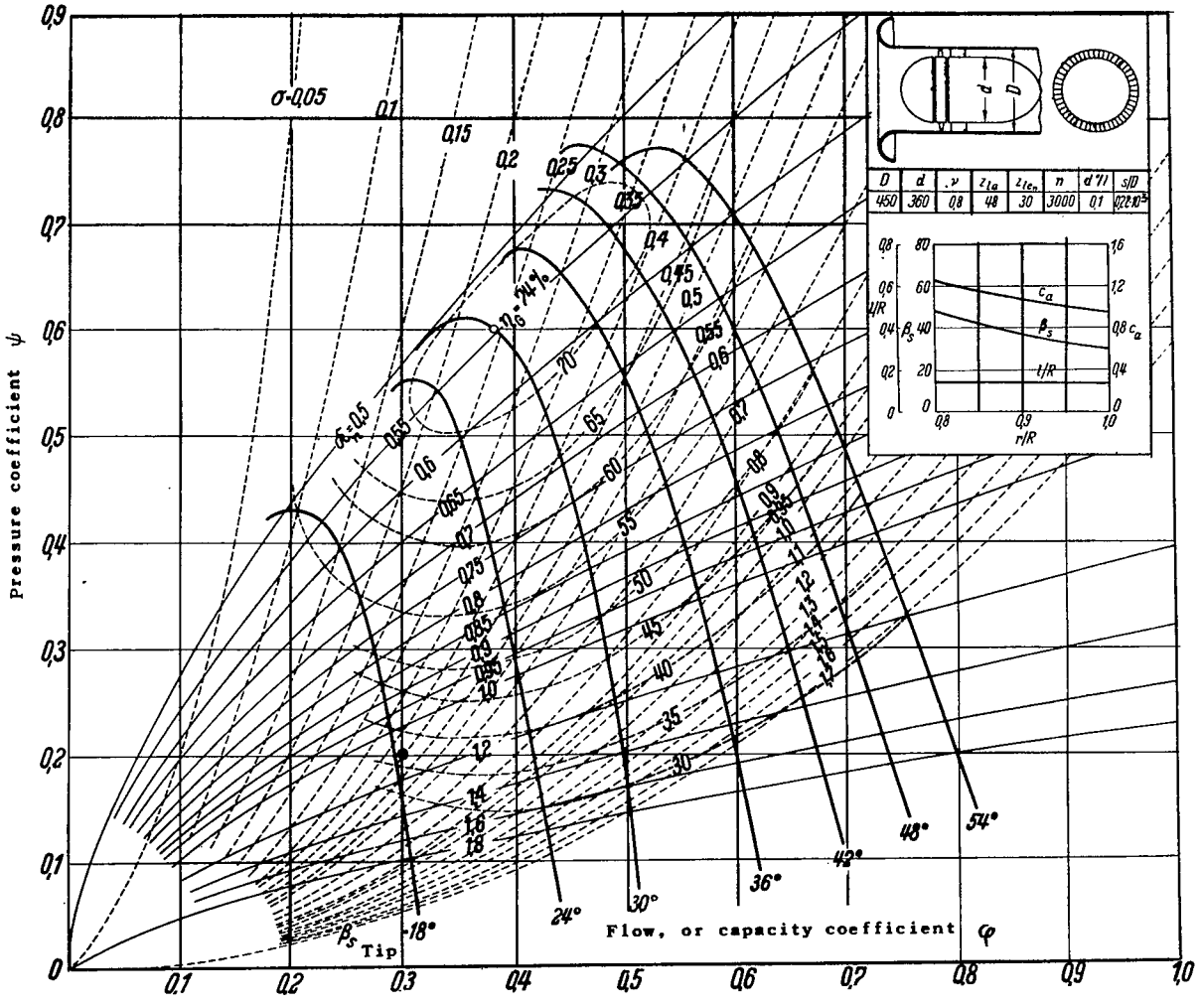

Figure 10.- Characteristics diagram of the test blower with lines of constant specific rotary speed K_n and constant throttling or quantity coefficients σ. Diameter ratio $\upsilon = 0.80$.

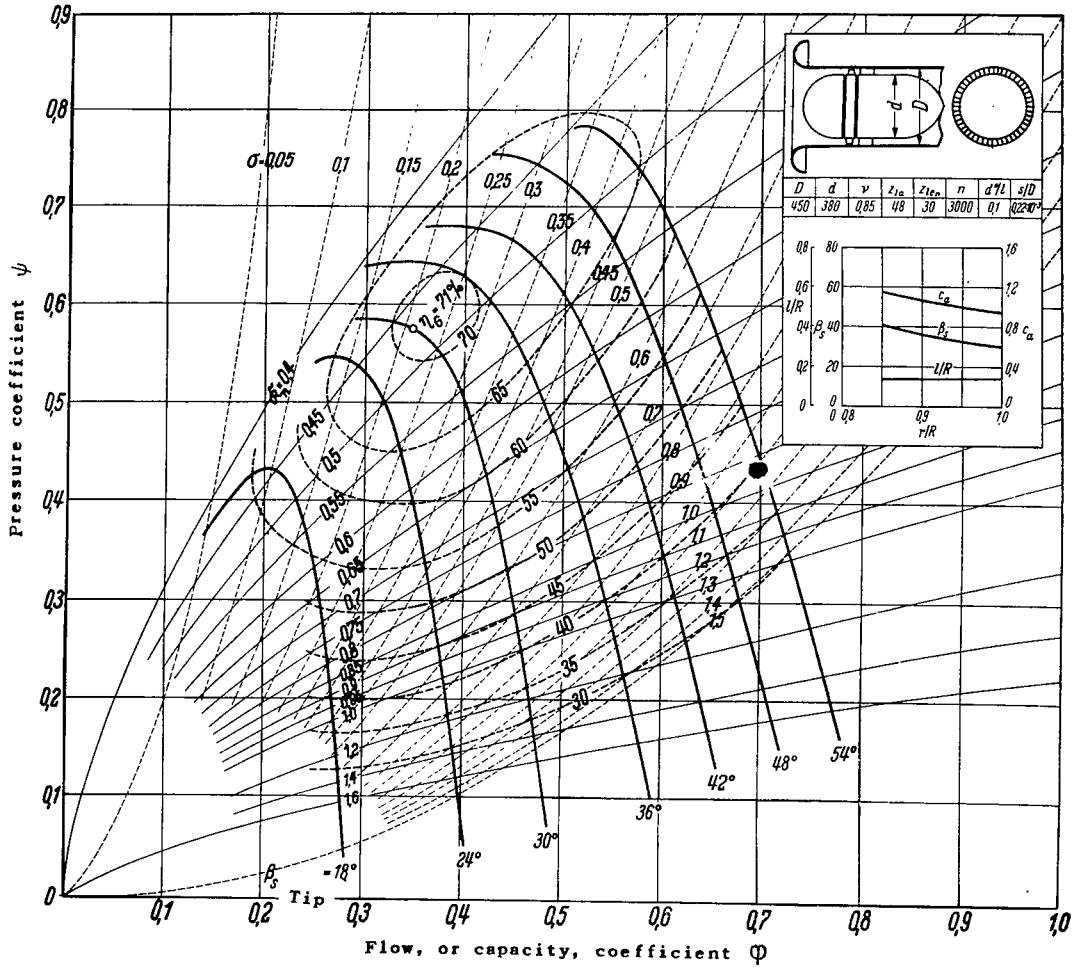

Figure 11.- Characteristics diagram of the test blower with lines of constant specific rotary speed K_n and constant throttling or quantity coefficients σ. Diameter ratio $\upsilon = 0.85$.

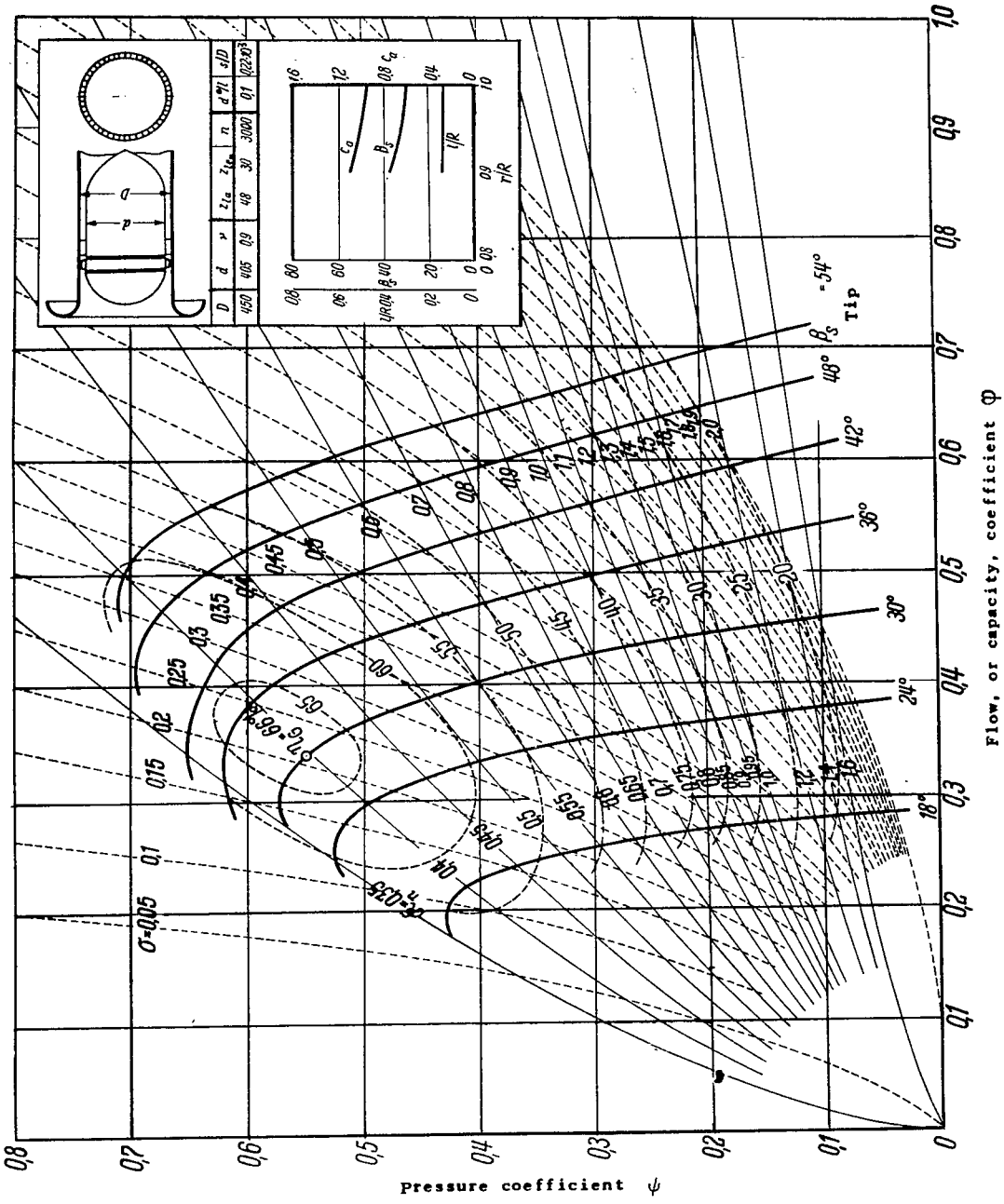

Figure 12.- Characteristics diagram of the test blower with lines of constant specific rotary speed K_n and constant throttling or quantity coefficients σ. Diameter ratio $\upsilon = 0.90$.

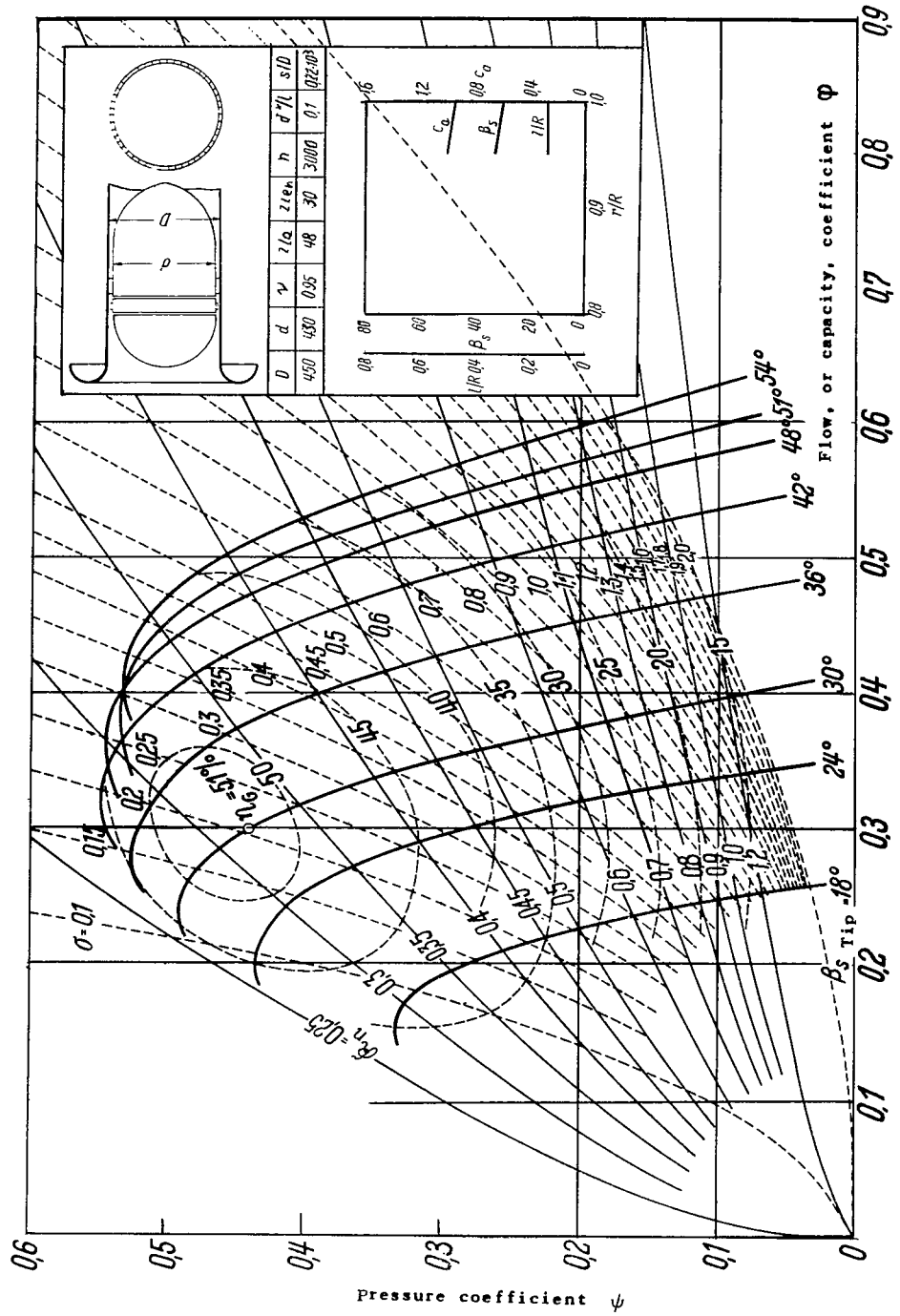

Figure 13.- Characteristics diagram of the test blower with lines of constant specific rotary speed and constant throttling or quantity coefficients σ. Diameter ratio $\upsilon = 0.95$.

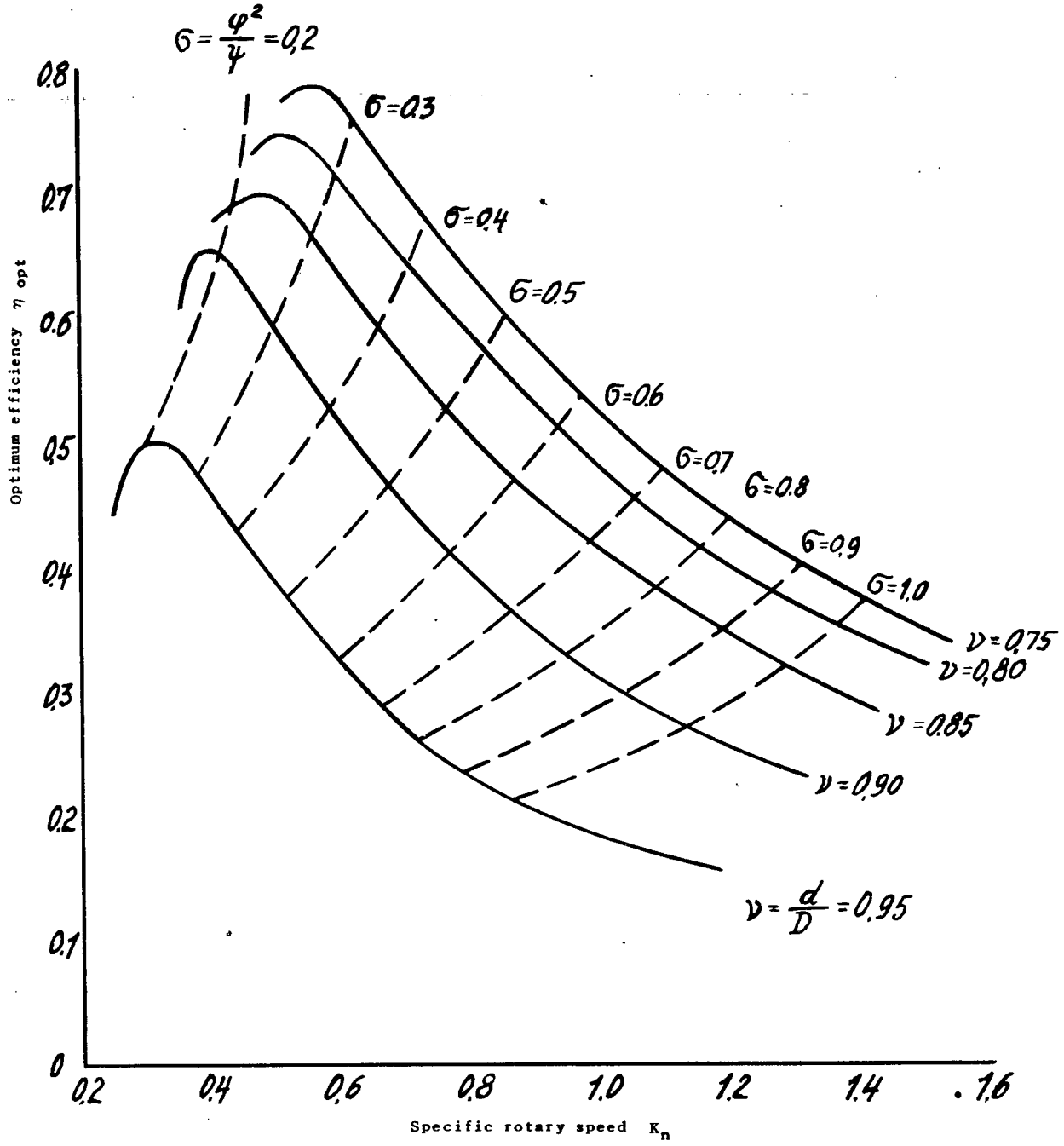

Figure 14.- Optimum efficiencies obtained as functions of the specific rotary speed, for various diameter ratios and lines of constant throttling or quantity coefficient.

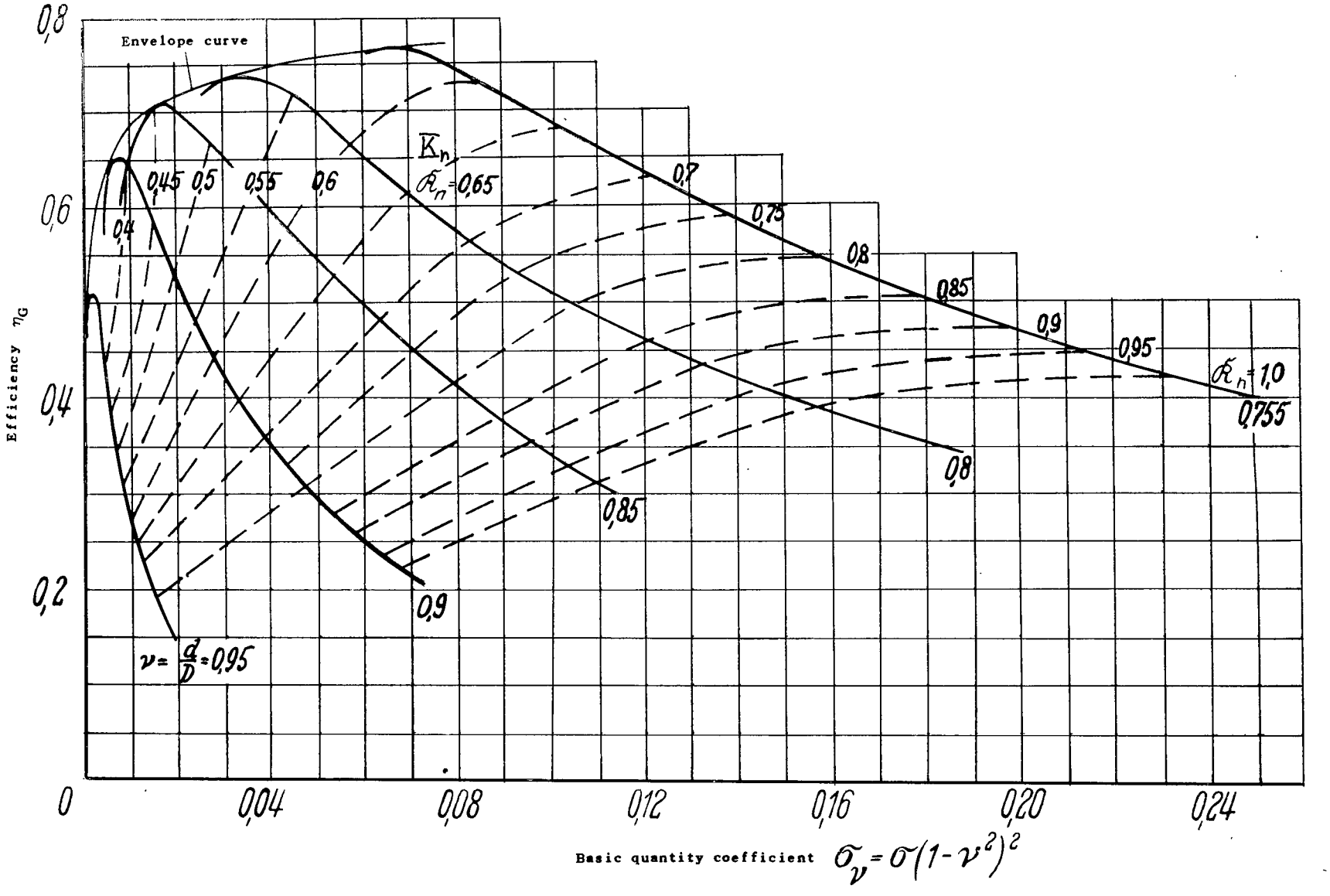

Figure 15.- Optimum efficiencies obtained as a function of basic throttling or quantity coefficient for various diameter ratio parameters. Specific speed is also plotted in dash lines.

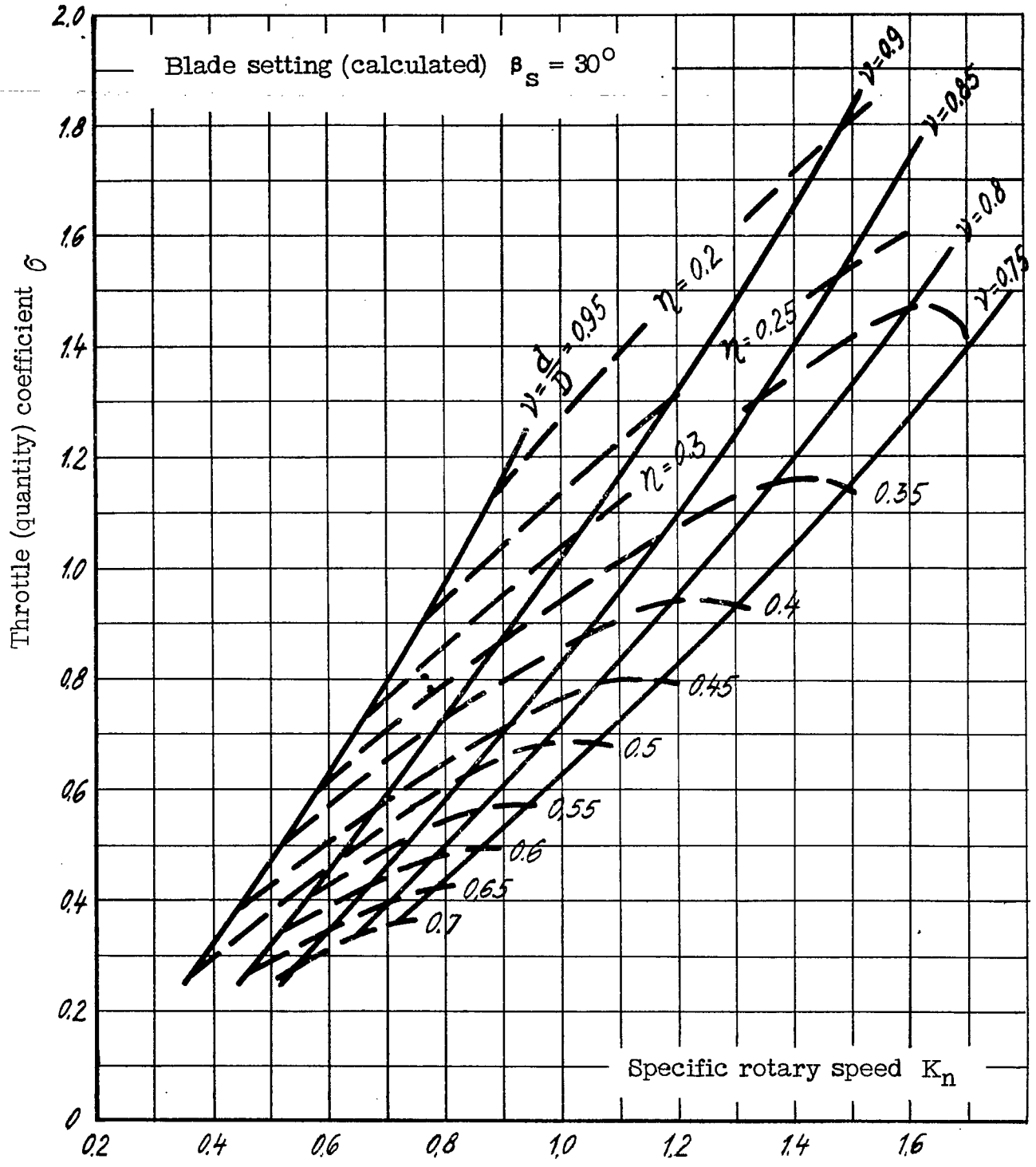

Figure 16.- Throttling or quantity coefficient σ as a function of the specific rotary speed K_n, for various diameter ratios υ and lines of constant efficiency (Calculation setting $\beta_s = 30°$).

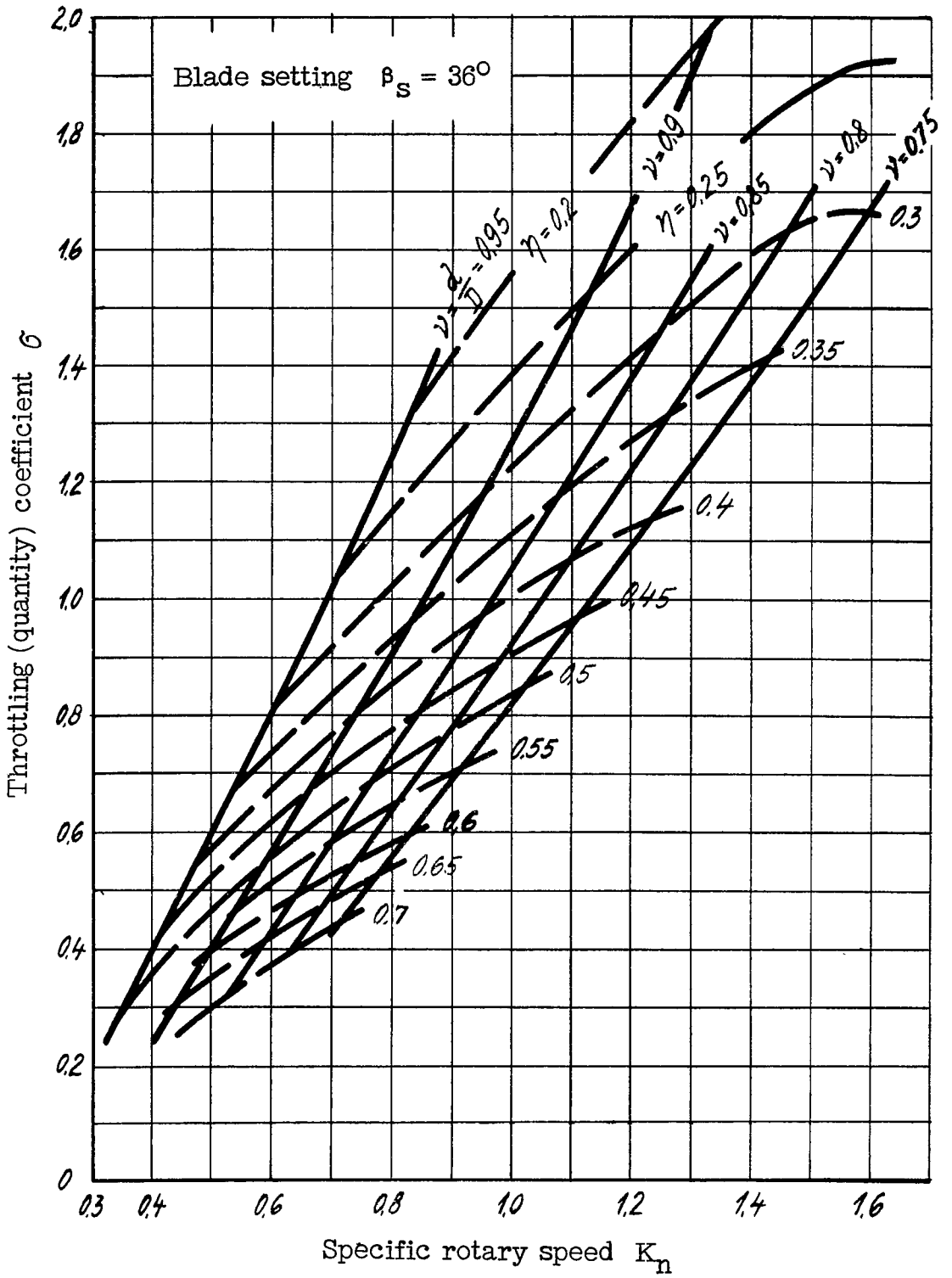

Figure 17.- Throttling or quantity coefficient σ as a function of the specific rotary speed K_n, for various diameter ratios and lines of constant efficiency ($\beta_s = 36^\circ$).

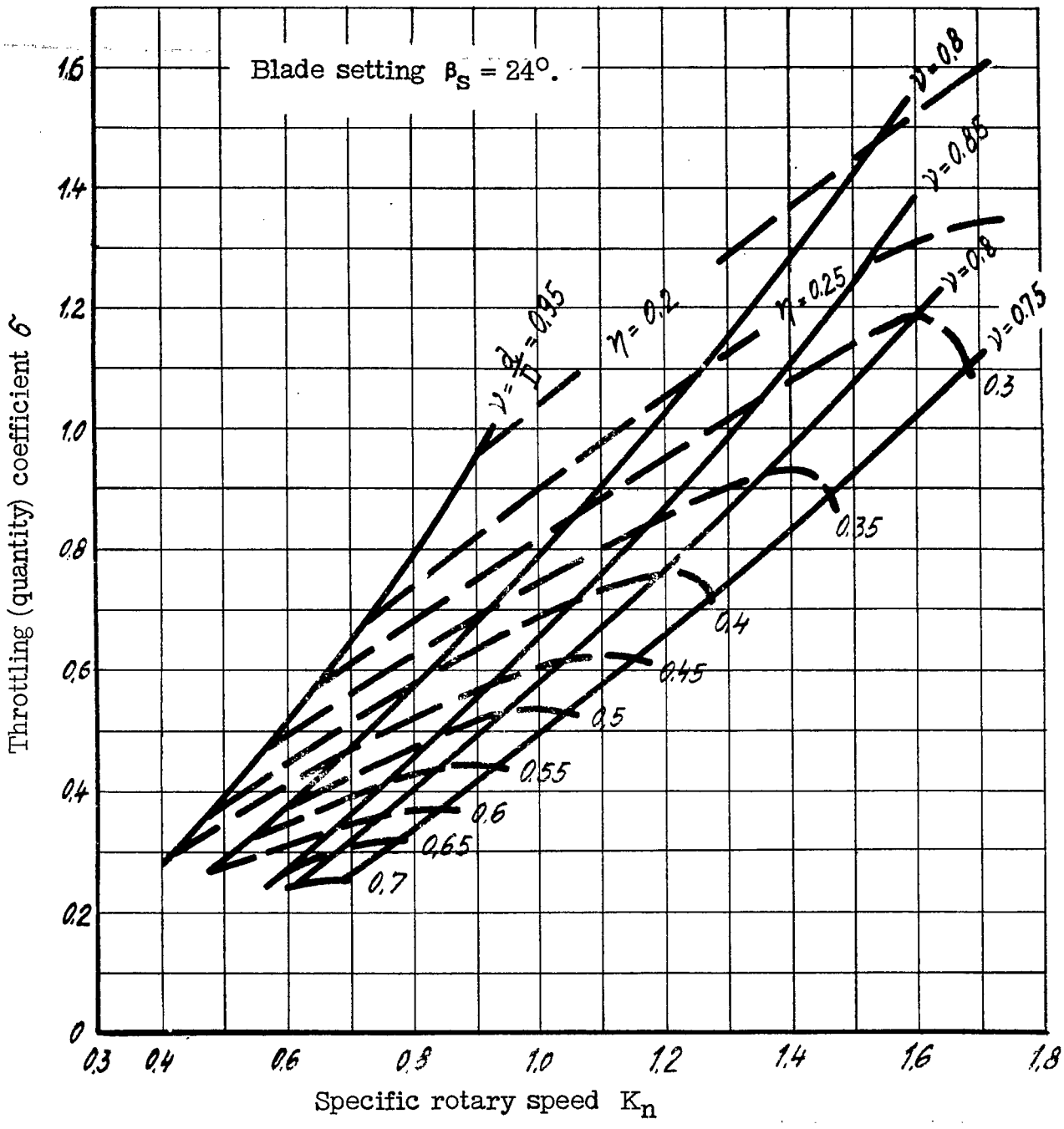

Figure 18.- Throttling or quantity coefficient σ as a function of the specific rotary speed K_n, for various diameter ratios and lines of constant efficiency ($\beta_s = 24^\circ$).

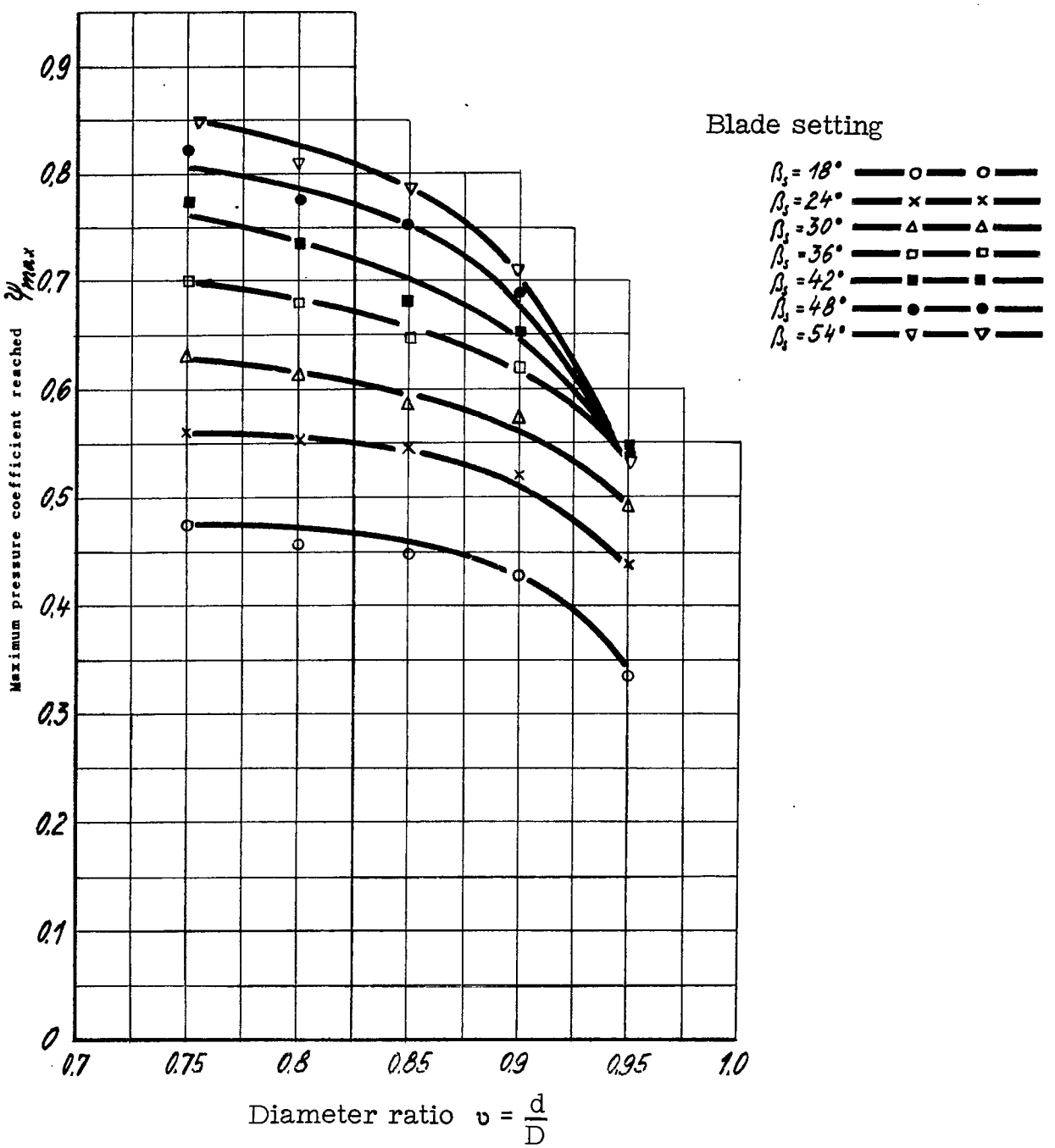

Figure 19.- The maximum blower pressure coefficients reached during the test for five different diameter ratios and seven different rotor blade settings.

Figure 20.- Ratio of the attainable pressure coefficient ($\psi_{max}\ \upsilon = x$) to the maximum pressure coefficient reached ($\psi_{max}\ \upsilon = 0.75$), as a function of the diameter ratio.

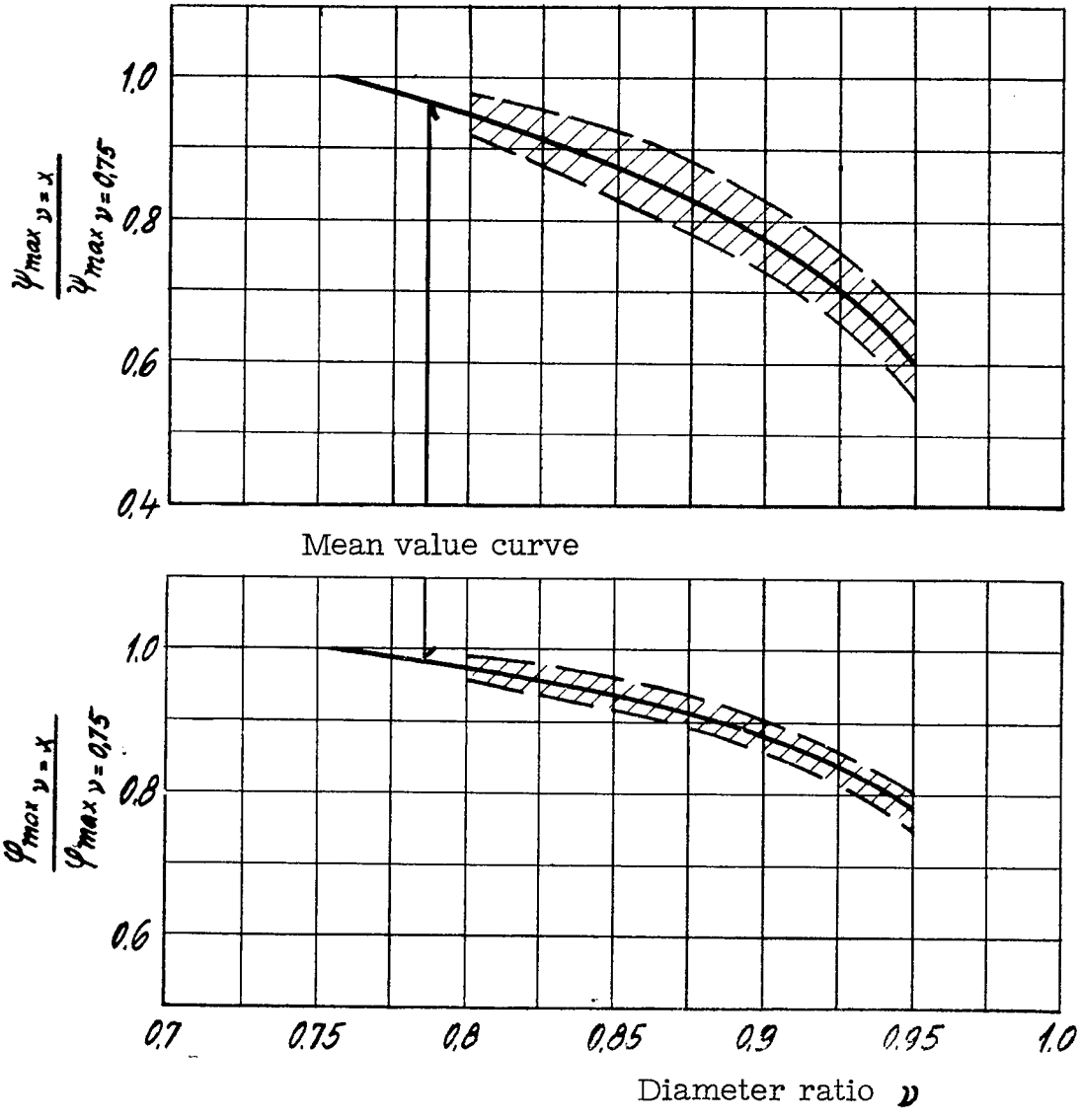

Figure 21.- Ratio of the attainable flow coefficient ($\varphi_{max}\ \upsilon = x$) to the maximum flow coefficient reached ($\varphi_{max}\ \upsilon = 0.75$), as a function of the diameter ratio.

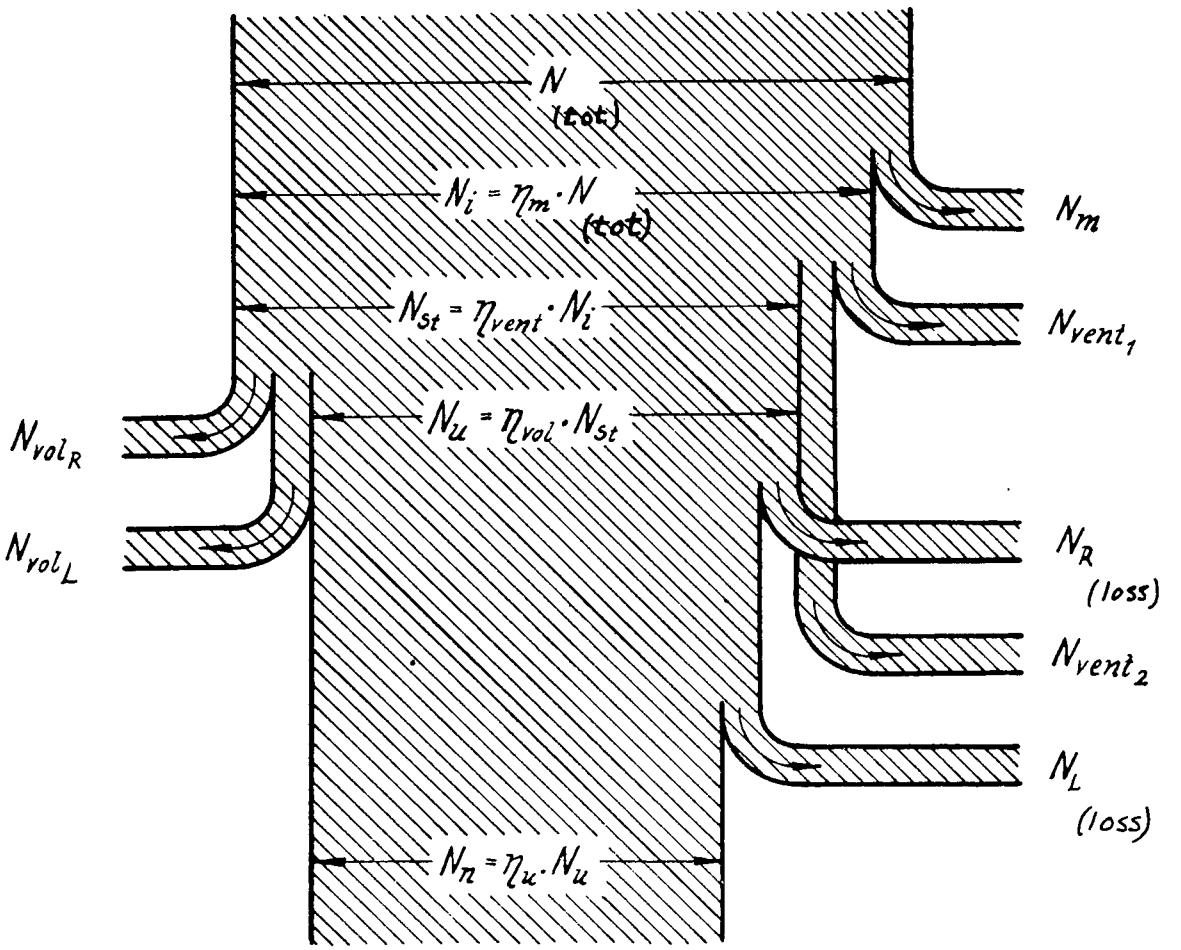

$$\eta_{ad} = \frac{N_n}{N_{(tot)}} = \eta_m \cdot \eta_{vent} \cdot \eta_{vol} \cdot \eta_u$$

Figure 22.- Energy balance of an axial flow compressor.

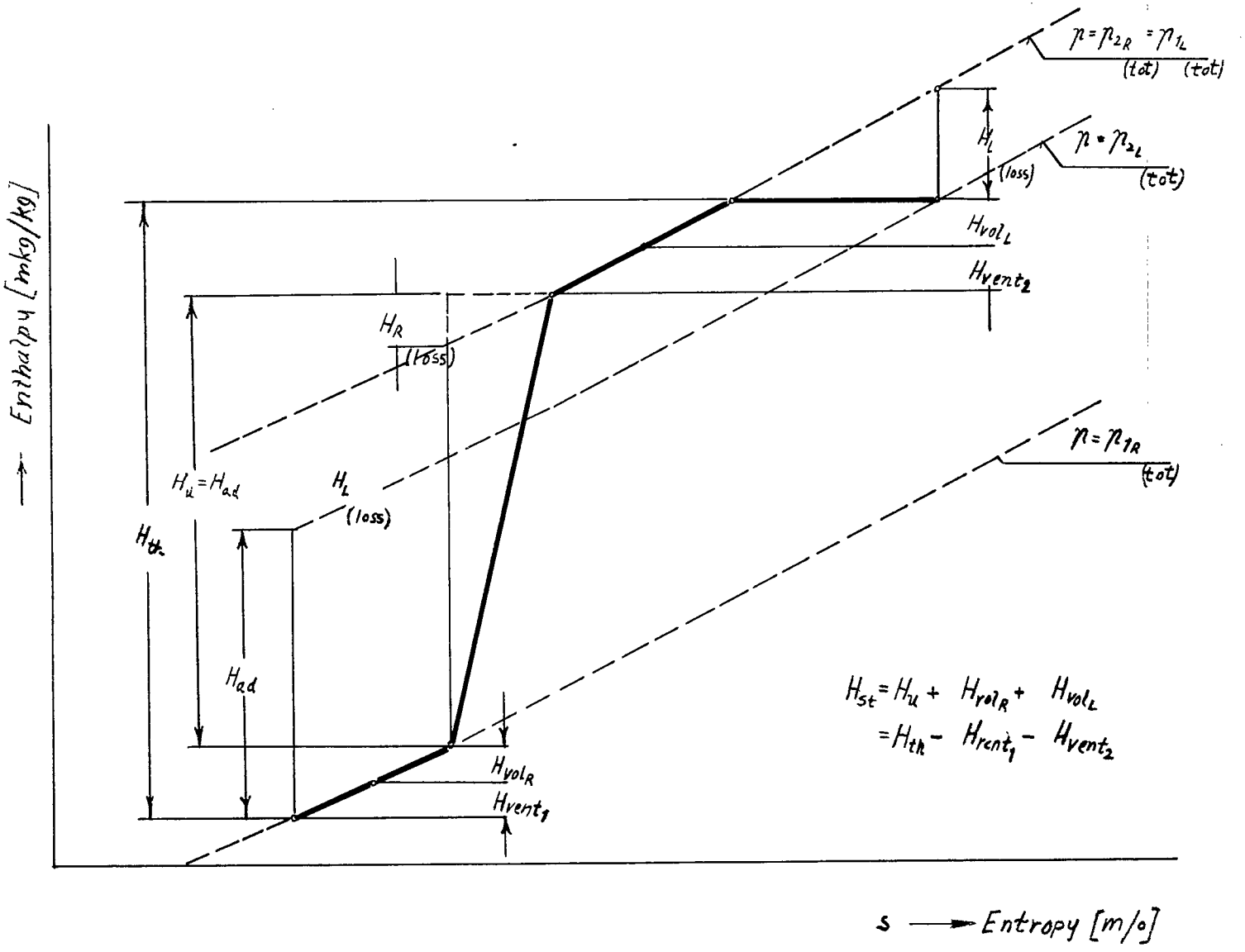

Figure 23.- Change of state of the air in flowing through the compressor.

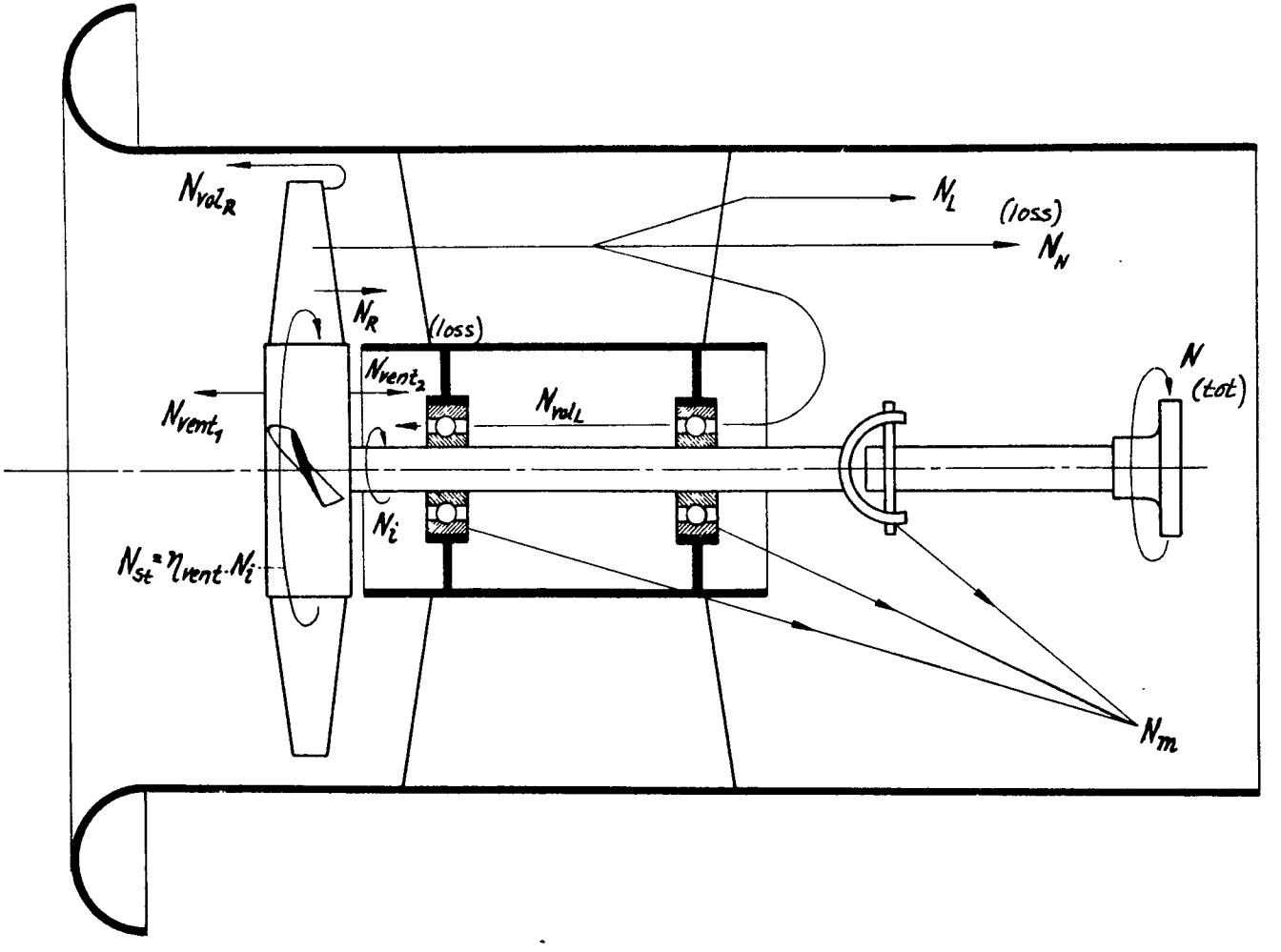

Figure 24.- Schematic representation of the sources of loss.

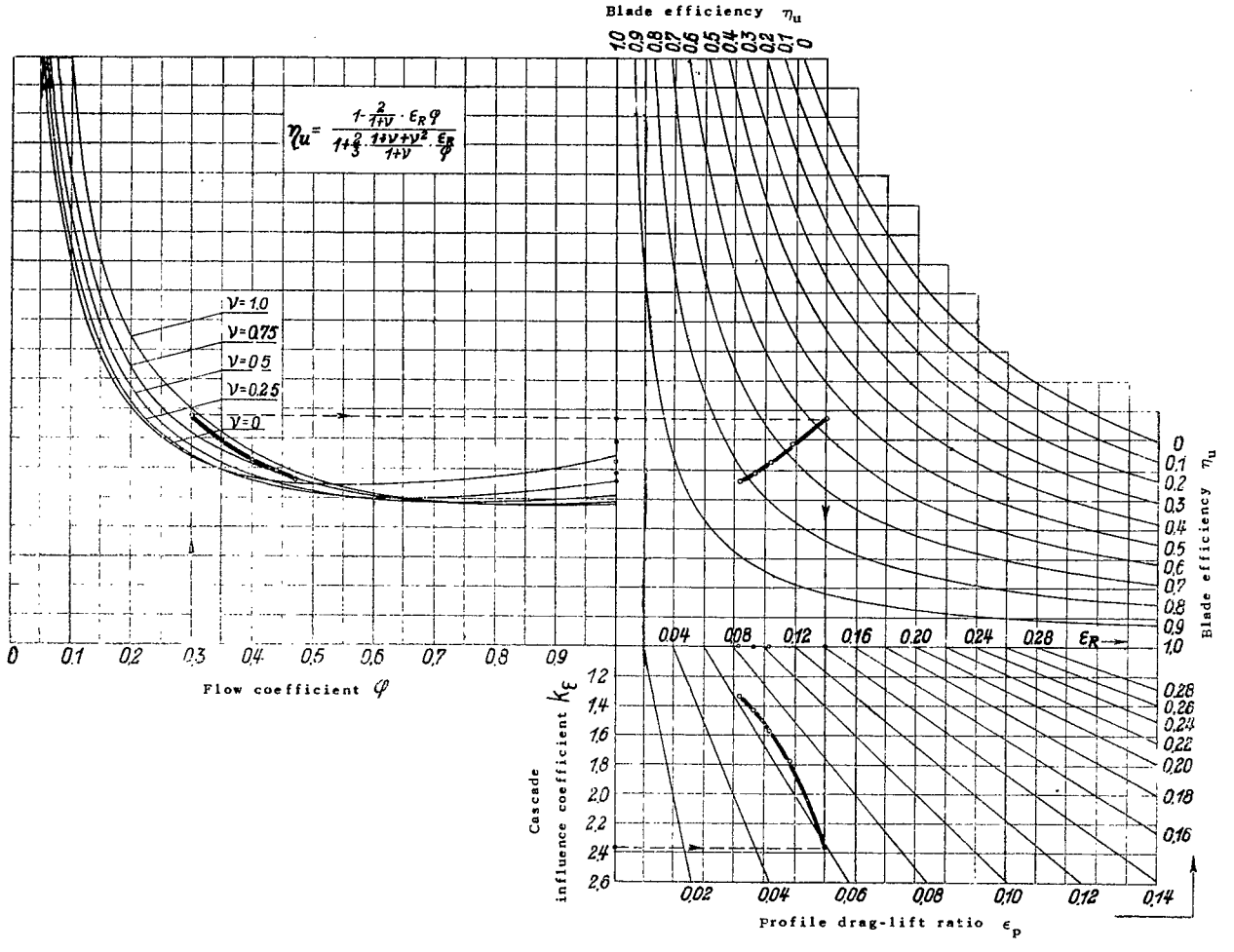

Figure 25.- Line diagram for the determination of any quantity in defining equation at top of page for given values of the other quantities. It is primarily used to determine profile drag-lift ratio from compressor.

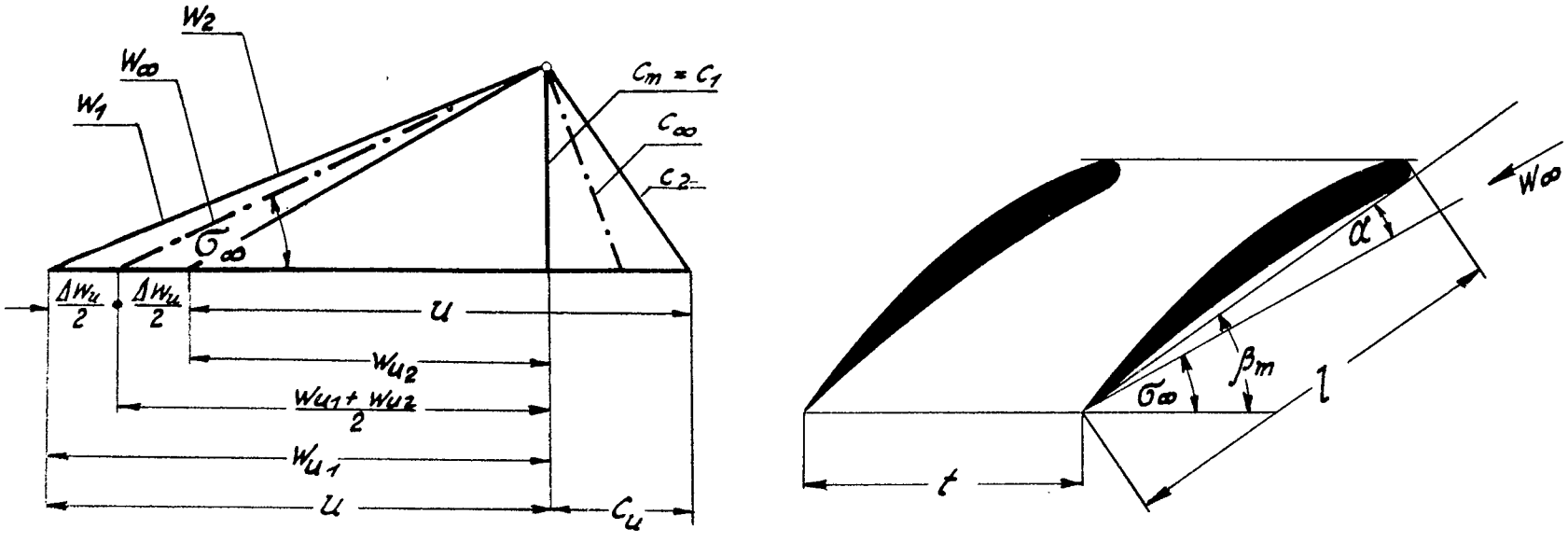

Figure 26.- Sketch explaining the symbols.

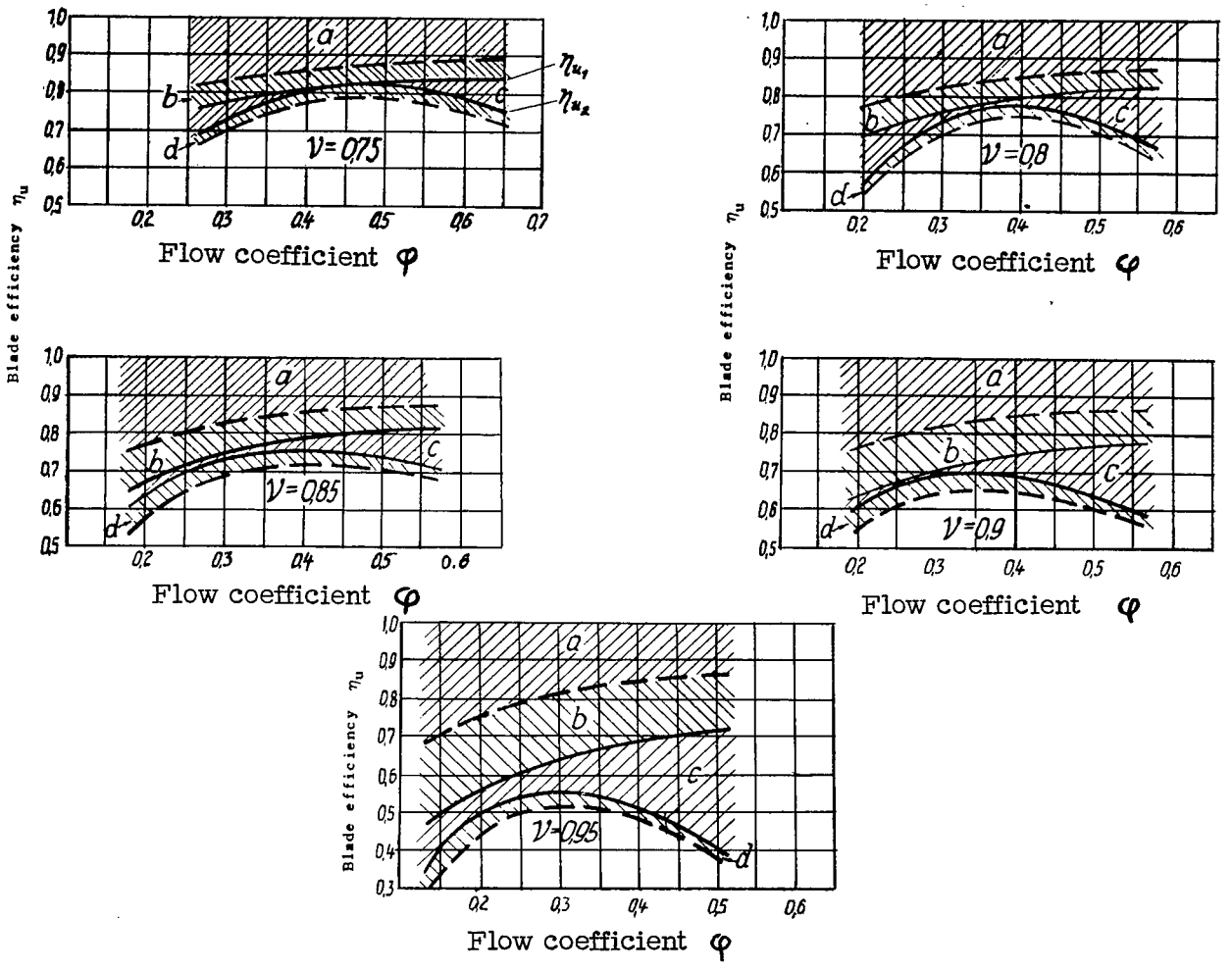

Figure 27.- Breakdown of blade efficiency η_u as a function of the flow coefficient φ for diameter ratios $\upsilon = 0.75$ to 0.95.

a. Losses as a result of friction at the acting surface of the blades. ($\epsilon p > 0$)
b. Friction losses at the hub and housing (guide surfaces) as a result of $k_\epsilon > 1$.
c. Losses still unexplained, possibly a result of entry shock in the following stator.
d. Clearance, windage and mechanical losses.